

# Cosmic strings lens phenomenology: General properties of distortion fields

Jean-Philippe Uzan

*Laboratoire de Physique Théorique, UMR-8627 du Centre National de la Recherche Scientifique, Université Paris XI, Bâtiment 210, F-91405 Orsay cedex, France*

*and Département de Physique Théorique, Université de Genève, 24 Quai E. Ansermet, CH-1211 Geneva 4, Switzerland*

Francis Bernardeau

*Service de Physique Théorique, CE de Saclay, F-91191 Gif-sur-Yvette, Cedex, France*

(Received 7 April 2000; published 29 December 2000)

We reconsider the general properties of gravitational lensing effects induced by cosmic string systems, taking into account their equation of state and motion equations. We explicitly show that the deflection patterns induced by a string is equivalent to the one of a static distribution of matter localized on a line. We then rigorously show that the convergence part of the deformation field is always zero, except on the intersection of the string world sheet and the observer past light cone, extending previous results obtained in peculiar cases. Phenomenological consequences of this result on multiple image systems are investigated.

DOI: 10.1103/PhysRevD.63.023004

PACS number(s): 98.80.Cq, 98.62.Sb, 98.80.Es, 98.80.Hw

## I. INTRODUCTION

It is well known that topological defects may appear whenever, in the thermal history of the universe, a symmetry breaking phase transition occurs [1,2], such as, for instance, in grand-unified theories [1] or in some extensions of the standard electro-weak model [3]. Such defects represent spacetime positions where the underlying order parameter cannot relax, because of topological constraints, to its low-energy vacuum state [1,4]. They are expected to interact mainly gravitationally with the ordinary matter so that they can induce (i) deflection and redshifting of massless particles, (ii) accretion of massive nonrelativistic particles, and (iii) emission of gravitational waves (see, e.g., Refs. [4–6] for a review of these effects).

One very interesting example, from a high-energy physics point of view as well as from a cosmological point of view, corresponds to the case of cosmic strings. In this case, their phenomenological properties are determined by the energy density per unit length of a string  $U$ . For instance, the deflection angle is of order  $4\pi GU$ ,  $G$  being the Newton constant. For defects formed at the grand-unification scale ( $T_{\text{GUT}} \sim 10^{16}$  GeV), we expect effects of a magnitude of  $GU \sim 10^{-6}$ . This corresponds, for instance, to the magnitude of the cosmic microwave background (CMB) anisotropies induced through the Kaiser-Stebbins effects [11]. Although topological defects may have clear observational signature on the CMB sky [11,12], observations seem to disfavor such an origin [7–10].

Nonetheless, this does not mean that topological defects do not exist. Their detection would be of dramatic importance both for astronomy and particle physics [1,4,6,13] since for instance, estimation or bounds on their density will help constrain the high-energy physics theories predicting their existence. Definitive predictions for string properties are, however, difficult to obtain because of the complex evolution equations that may depend on their microscopic structure through their equation of state. For the so-called Goto-Nambu strings (where the energy per unit length  $U$  and the

tension  $T$  of the string are equal), it was shown that the spacetime around such straight cosmic string was conical [14–18]. Such a cosmic string formed at a grand unified theory (GUT) scale would therefore induce image pairs of distant objects with angular separation of order  $\theta \sim 5.2'' \times (GU/10^{-6})$ . From a pure phenomenological point of view such a string is expected to produce lines of double images [19]. Recognizing the peculiarity of such a system, it was later extended to straight cosmic string with different equation of state [20,21] and to a string with a lightlike current pulse [22]. Moreover numerical simulations for a Goto-Nambu string were also performed in the case of long strings [23] and cosmic loops [24,25]. More quantitatively the prospects for a direct detection of relic string via gravitational lensing, and in particular the expected number of events, was first discussed by Hindmarsh [19] who estimated the angular length of string per unit area on the sky out to a redshift  $z$  to be of order

$$\theta_{\text{loops}} \sim 0.1 \nu z^2 \text{ deg.}^{-1}, \quad \theta_{\text{long string}} \sim 0.1 A z^2 \text{ deg.}^{-1},$$

where  $\nu$  and  $A$  are two coefficients of order unity (see also Ref. [23]). In conclusion, it is widely believed that the observation of a cosmic string can be achieved through double image detections, although, in practice, it might be difficult to be positive about such a detection since pairs with the same angular separation appearing by pure coincidence can be very high (as pointed by Cowie and Hu who reported for such a cosmic string lens candidate [26,27]).

The aim of this article and its companion [28] is to make a systematic investigation of the gravitational lensing effects by cosmic strings. We focus our analysis on the deformation equation of a geodesic bundle in presence of cosmic strings (Sec. II). Standard approximations of the gravitational lens theory are also discussed in this section. After a description of the cosmic string dynamics in Sec. III, we show in Sec. IV that the deflecting potential of a cosmic string is equivalent to the one by a static distribution of matter on the projection of the string world sheet onto the observer past light cone. In

the course in this calculation we show that the deformation field induced by cosmic strings has a zero convergence (without any approximation). Examples illustrating these results are discussed as well as the validity of the thin lens approximation and the influence of the equation of state. In Sec. V we investigate the phenomenological consequences of the zero convergence property on multiple image systems. In Ref. [28] we propose a phenomenological model of string energy distribution that gives a more quantitative account of these results.

## II. EVOLUTION OF A LIGHT BEAM

In lens systems that are usually considered in cosmology, such as galaxies or galaxy clusters, the metric perturbations correspond to those of scalar perturbations. This is not the case for cosmic string effects where relativistic motions, nontrivial equation of state, also induce vector and tensor perturbations. We are thus forced to consider the deformation equations of light beams in their full generality. In the geometric optic approximation, an electromagnetic plane wave propagating in an arbitrary spacetime  $\mathcal{M}$  without interaction with matter can be described by a null geodesic [29]. The goal of this section is to review the description of the evolution and distortion of a bundle of null geodesics and we start by introducing the standard elements of the gravitational lensing theory and then apply them to a perturbed spacetime. We then discuss the thin lens approximation and finish by some comments on its applicability.

### A. Basics of gravitational lensing

We consider a bundle of null geodesics  $g$  propagating in a spacetime  $\mathcal{M}$ . Each geodesic can be described as

$$g: \quad x^\mu(\lambda) = \bar{x}^\mu(\lambda) + \xi^\mu(\lambda), \quad (1)$$

where  $\bar{x}^\mu(\lambda)$  is the equation of a geodesic  $g_0$  chosen as reference and  $\xi^\mu$  is a displacement vector labeling the other geodesics with respect to  $g_0$ . Greek indices run from 0 to 3 and  $\lambda$  is an affine parameter along the geodesic  $g_0$ . With these notations, we can define the tangent vector to  $g_0$  by

$$k^\mu \equiv \frac{d\bar{x}^\mu}{d\lambda}. \quad (2)$$

It is a null vector satisfying the geodesic equation, i.e., solution of

$$k_\mu k^\mu = 0, \quad k^\mu \nabla_\mu k^\nu = 0, \quad (3)$$

where  $\nabla_\mu$  is the covariant derivative associated to the metric  $g_{\mu\nu}$  the signature of which will be chosen as  $(-, +, +, +)$ .

Now, we consider such a bundle converging at a point  $O \in \mathcal{M}$  where we assume that there is an observer with 4-velocity  $u^\mu$  ( $u^\mu$  is a timelike vector, i.e., such that  $u^\mu u_\mu = -1$ ) and we choose the affine parameter  $\lambda$  to vanish at  $O$  and to increase toward the past. We then consider at  $O$  the basis  $(k^\mu, u^\mu, n_1^\mu, n_2^\mu)$  where  $n_{1,2}^\mu$  are two spacelike vectors ( $n_a^\mu n_{a\mu} = +1$ ,  $a = 1, 2$ ) such that

$$n_1^\mu n_{2\mu} = 0, \quad k_\mu n_a^\mu = 0, \quad \text{and} \quad u_\mu n_a^\mu = 0 \quad (4)$$

and  $k^\mu$  is the null vector defined in Eq. (2). Starting from this basis at  $O$ , we construct such a basis at any point of the light ray world line  $\bar{x}^\mu$  by parallel transporting it as

$$k^\mu \nabla_\mu X^\nu = 0 \quad (5)$$

for  $X = u, n_1$ , and  $n_2$ . Note that since  $k^\mu$  satisfies Eq. (3) this implies that Eq. (5) is in fact the Fermi-Walker transport and thus  $u, n_1$ , and  $n_2$  remain orthonormal and satisfy Eq. (4) for all  $\lambda$ . Since the tangent vector  $k_g^\mu \equiv k^\mu + d\xi^\mu/d\lambda$  to each geodesic  $g$  of the bundle is a null vector, we deduce from  $k_g^\mu k_{g\mu} = g_{\mu\nu}(\bar{x}^\alpha + \xi^\alpha)k_g^\mu k_g^\nu = 0$  that  $2k_\mu d\xi^\mu/d\lambda + k^\mu k^\nu \xi^\alpha \partial_\alpha g_{\mu\nu} = 0$  at first order in  $\xi$ . It can then be concluded that, using Eq. (5),  $k_\mu \xi^\mu$  is constant along the geodesic and vanishes at  $O$  so that it can be decomposed as

$$\xi^\mu = \xi_0 k^\mu + \sum_{a=1,2} \xi_a n_a^\mu. \quad (6)$$

$\xi_0$  does not vanish in general, but two such decompositions (6) with different  $\xi_0$  parametrize the same light ray. We can, for instance, impose that  $\xi^\mu$  is spatial for the observer with 4-velocity  $u^\mu$  (i.e.,  $k_\mu u^\mu = 0$ ) which then fixes the value of  $\xi_0$ . We also decompose the coordinates of every event of  $\mathcal{M}$  in the neighborhood of  $g_0$  as

$$x^\mu = \lambda k^\mu + \sum_{a=1,2} x_a n_a^\mu + \tau u^\mu. \quad (7)$$

The equation of evolution of  $\xi^\mu$  is obtained by writing the geodesic deviation equation [29]

$$\frac{D^2}{d^2\lambda} \xi^\mu = R^\mu_{\nu\alpha\beta} k^\nu k^\alpha \xi^\beta, \quad (8)$$

where  $R_{\mu\nu\alpha\beta}$  is the Riemann tensor of the metric  $g_{\mu\nu}$  and where  $D/d\lambda \equiv k^\nu \nabla_\nu$ . Inserting the decomposition (6) in Eq. (8) and using the fact that  $\xi_a = n_a^\mu \xi_\mu$  is a scalar (so that  $D\xi_a/d\lambda = d\xi_a/d\lambda$  with  $d/d\lambda \equiv k^\mu \partial_\mu$ ) leads to

$$\ddot{\xi}_a = \mathcal{R}_a^b \xi_b, \quad (9)$$

where  $\mathcal{R}_{ab} \equiv R_{\mu\nu\alpha\beta} k^\nu k^\alpha n_a^\mu n_b^\beta$  and an overdot refers to a derivation with respect to  $\lambda$ . Due to the linearity of the geodesic deviation equation (9),  $\xi_a$  can be related to its initial value  $\xi_a(0)$  through a linear transformation  $\mathcal{D}_{ab}$  as

$$\xi_a(\lambda) \equiv \mathcal{D}_a^b(\lambda) \xi_b(0). \quad (10)$$

Since  $\xi(0) = 0$  for a bundle converging at  $O$ , with two derivatives (10) and using this equation again to eliminate  $\xi(0)$ , we obtain the equation of evolution for  $\mathcal{D}_{ab}$

$$\ddot{\mathcal{D}}_{ab} = \mathcal{R}_a^c \mathcal{D}_{cb} \quad (11)$$

with initial conditions

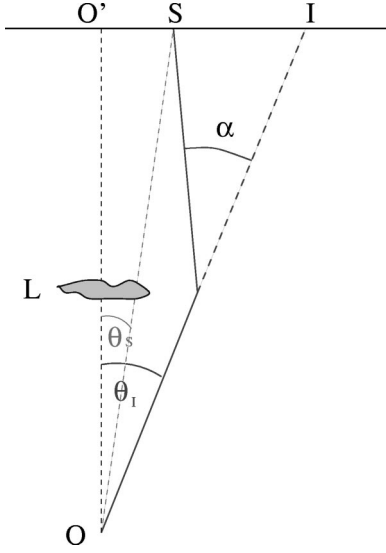


FIG. 1. Description of the lensing geometry.  $S$  is the source,  $L$  the lens, and  $I$  the image of  $S$ .  $O'S \equiv \xi(\lambda_S)$ .

$$\mathcal{D}_{ab}(0)=0 \text{ and } \dot{\mathcal{D}}_{ab}(0)=I_{ab}, \quad (12)$$

$I_{ab}$  being the  $2 \times 2$  identity matrix. This equation has been derived in e.g., Refs. [30–33].  $\mathcal{D}_{ab}$  characterizes the deformation field while looking in different directions. Quoting that  $\dot{\xi}(0) \equiv \theta_l$  is the vectorial angle of observation and  $\xi(\lambda_S) \equiv \lambda_S \theta_s$  where  $\theta_s$  is the vectorial angular position of the source, Eq. (10) can be rewritten in terms of these angles (see Fig. 1) as

$$\theta_s^a = \frac{\mathcal{D}_b^a(\lambda_S)}{\lambda_S} \theta_l^b. \quad (13)$$

The amplification matrix  $\mathcal{A}_b^a \equiv d\theta_s^a/d\theta_l^b$  can be expressed in terms of  $\mathcal{D}$  as

$$\mathcal{A}_b^a = \frac{\mathcal{D}_b^a(\lambda_S)}{\lambda_S}. \quad (14)$$

In the following, we decompose it in terms of convergence  $\kappa$  and shear  $\vec{\gamma} \equiv (\gamma_1, \gamma_2)$  as

$$\mathcal{A}_{ab} = \begin{pmatrix} 1 - \kappa - \gamma_1 & \gamma_2 \\ \gamma_2 & 1 - \kappa + \gamma_1 \end{pmatrix}. \quad (15)$$

### B. Application to a perturbed spacetime

We now restrict our study to a perturbed spacetime of metric

$$ds^2 = g_{\mu\nu} dx^\mu dx^\nu \equiv (\eta_{\mu\nu} + h_{\mu\nu}) dx^\mu dx^\nu, \quad (16)$$

with  $\eta_{\mu\nu}$  being the Minkowski metric  $\eta_{\mu\nu} = \text{diag}(-, +, +, +)$ . We work in harmonic gauge

$$\partial_\nu h^{\mu\nu} = 0, \quad (17)$$

so that the Ricci tensor at linear order in the perturbation  $h_{\mu\nu}$  reduces to

$$R_{\mu\nu} = \frac{1}{2}(\partial_i^2 - \Delta)h_{\mu\nu}, \quad (18)$$

$\Delta$  being the Laplacian  $\Delta \equiv \partial_i \partial^i$ , Latin indices running from 1 to 3. The Einstein equations take the simple form

$$(\partial_i^2 - \Delta)h_{\mu\nu} = 16\pi G \left( T_{\mu\nu} - \frac{1}{2} \eta_{\mu\nu} T^\lambda{}_\lambda \right) \equiv 16\pi G \mathcal{F}_{\mu\nu}, \quad (19)$$

$T_{\mu\nu}$  being the stress-energy tensor of the matter perturbation.

The solution of this equation can be obtained by means of the Green functions  $\mathcal{G}^{(\pm)}$  of the d'Alembertian [34]

$$(\Delta_x - \partial_t^2) \mathcal{G}^{(\pm)}(\vec{x}', t', \vec{x}, t) = \delta^{(3)}(\vec{x} - \vec{x}') \delta(t - t')$$

$\Leftrightarrow$

$$\mathcal{G}^{(\pm)}(\vec{x}', t', \vec{x}, t) = -\frac{1}{4\pi} \frac{\delta(t' - t \pm |\vec{x} - \vec{x}'|)}{|\vec{x} - \vec{x}'|}, \quad (20)$$

so that, using the retarded solution, we solve the Einstein equations (18) at linear order as

$$h_{\mu\nu}(\vec{x}, t) = 4G \int \frac{d^3 \vec{x}'}{|\vec{x} - \vec{x}'|} \mathcal{F}_{\mu\nu}(\vec{x}', t - |\vec{x} - \vec{x}'|). \quad (21)$$

Now, we can solve Eq. (11) order by order: at zeroth order,  $\mathcal{R}_{ab} = 0$  so that it reduces trivially to

$$\mathcal{D}_{ab}^{(0)}(\lambda) = \lambda I_{ab}; \quad (22)$$

at first order, the equation of evolution (11) gives

$$\dot{\mathcal{D}}_{ab}^{(1)}(\lambda) = \lambda \mathcal{R}_{ab}^{(1)}(\lambda) \quad (23)$$

from which we deduce that  $\mathcal{D}_{ab}^{(1)}(\lambda)$  is given by

$$\mathcal{D}_{ab}^{(1)}(\lambda_S) = \int_0^{\lambda_S} \lambda (\lambda_S - \lambda) \mathcal{R}_{ab}^{(1)}(\lambda) d\lambda. \quad (24)$$

It is interesting to note that while  $\mathcal{D}_{ab}$  is not symmetric in general, it is symmetric at first order in the perturbation.

Using the expression of the Riemann tensor as  $2R_{\mu\sigma\nu\rho} = h_{\sigma\nu,\mu\rho} + h_{\mu\rho,\sigma\nu} - h_{\nu\mu,\sigma\rho} - h_{\sigma\rho,\nu\mu}$ , we obtain

$$\mathcal{R}_{ab}^{(1)} = \frac{1}{2} h_{\nu\sigma,\mu\rho} k^\nu k^\sigma n_a^\mu n_b^\rho - \frac{1}{2} \frac{d}{d\lambda} (\Gamma_{\rho\beta}^\alpha \eta_{\alpha\mu} k^\beta n_a^\mu n_b^\rho), \quad (25)$$

where  $k^\mu$ ,  $n_1^\mu$ , and  $n_2^\mu$  are evaluated on the unperturbed geodesic (and are thus constant) and where  $\Gamma_{\rho\beta}^\alpha$  are the Christoffel symbols at first order in the perturbation. Choosing

$$n_a^\mu \equiv \delta_a^\mu \quad (26)$$

and defining the deflecting potential  $\Phi$  as

$$\Phi(\vec{x}, t) \equiv \frac{1}{2} h_{\mu\nu} k^\mu k^\nu, \quad (27)$$

where  $t(\lambda) = t_0 - x_{\parallel}(\lambda)$  is the equation of the photon trajectory [ $t_0$  is the time of the observation  $t_0 = t(\lambda = 0)$ ], we obtain

$$\begin{aligned} \mathcal{D}_{ab}^{(1)}(x_a, \lambda_S) = & \left( \int_0^{\lambda_S} \lambda(\lambda_S - \lambda) \partial_{ab} \Phi[x_a, x_{\parallel}(\lambda), t(\lambda)] d\lambda \right) \\ & + \int_0^{\lambda_S} \lambda(\lambda_S - \lambda) \Psi_{ab}[x_a, x_{\parallel}(\lambda), t(\lambda)] d\lambda, \end{aligned} \quad (28)$$

where

$$\Psi_{ab}(\vec{x}, t) \equiv -\frac{1}{2} \frac{d}{d\lambda} (\Gamma_{a\beta}^\alpha \eta_{ab} k^\beta) \quad (29)$$

and where  $\partial_a$  refers to a derivative with respect to the coordinates  $x_a$  as defined in Eq. (7).

### C. The thin lens approximation for static distribution of matter

In the thin lens approximation, one assumes that the effect of the deflecting body takes place over only a small fraction of the light path. This approximation is usually considered in cases of scalar perturbations. The aim of this section is to recall its derivation in the standard case to see to which extent it applies for cosmic strings. We thus assume that the lens is localized at  $\lambda = \lambda_L$  with an extension small compared to  $\lambda_L$  and that this matter distribution is static so that  $\mathcal{F}_{\mu\nu} k^\mu k^\nu \equiv \Sigma[\vec{x}_\perp, x_{\parallel}(\lambda_L)] \delta[x_{\parallel}(\lambda) - x_{\parallel}(\lambda_L)]$ , where  $\Sigma$  is the surface energy density. It follows that the deflecting potential reduces, after integration over the direction of propagation, to

$$\begin{aligned} \Phi(\vec{x}_\perp, x_{\parallel}) = & 2G \\ & \times \int \frac{d^2 \vec{x}'_\perp}{\sqrt{|\vec{x}_\perp - \vec{x}'_\perp|^2 + [x_{\parallel} - x_{\parallel}(\lambda_L)]^2}} \Sigma[\vec{x}'_\perp, x_{\parallel}(\lambda_L)], \end{aligned} \quad (30)$$

where  $\vec{x}_\perp \equiv (x_1, x_2)$ . Since only  $\partial_{ab} \Phi$  enters the expression of  $\mathcal{D}_{ab}^{(1)}$  and since this quantity varies as  $[x_{\parallel} - x_{\parallel}(\lambda_L)]^{-3}$  as soon as we are looking close to the string (i.e., when  $|\vec{x}_\perp - \vec{x}_{\perp,L}| \ll [x_{\parallel} - x_{\parallel}(\lambda_L)]$ ) we can approximate the deflecting potential as

$$\Phi(\vec{x}) = \tilde{\Phi}(\vec{x}_\perp) \delta[x_{\parallel} - x_{\parallel}(\lambda_L)] \quad (31)$$

with

$$\begin{aligned} \tilde{\Phi}(\vec{x}_\perp) & \equiv \int_0^{\lambda_S} \Phi[\vec{x}_\perp, x_{\parallel}(\lambda)] d\lambda \\ & = 2G \int \Sigma[\vec{x}'_\perp, x_{\parallel}(\lambda_L)] [\ln|x_{\parallel}(\lambda) - x_{\parallel}(\lambda_L)| \\ & \quad + \sqrt{(\vec{x}_\perp - \vec{x}'_\perp)^2 + [x_{\parallel}(\lambda) - x_{\parallel}(\lambda_L)]^2}]_0^{\lambda_S} d^2 \vec{x}'_\perp. \end{aligned} \quad (32)$$

Now, if we assume that the impact parameter is small compared to the two distances lens object and observer lens, i.e.,

$$|\vec{x}_\perp - \vec{x}_{\perp,L}| \ll [x_{\parallel}(\lambda_S) - x_{\parallel}(\lambda_L), x_{\parallel}(\lambda_L)], \quad (33)$$

we deduce that the deflecting potential integrated along the line of sight is given by

$$\tilde{\Phi}(\vec{x}_\perp) = -4G \int \ln|\vec{x}_\perp - \vec{x}'_\perp| \Sigma[\vec{x}'_\perp, x_{\parallel}(\lambda_L)] d^2 \vec{x}'_\perp \quad (34)$$

up to a constant which depends only on  $x_{\parallel}(\lambda_L)$  and  $x_{\parallel}(\lambda_S)$ ; we forget this constant since  $\mathcal{D}_{ab}$  involving only derivatives of  $\tilde{\Phi}$  and is thus independent of its value. The second contribution of  $\mathcal{D}_{ab}^{(1)}$  involves the computation of the potential  $\Psi_{ab}$  and one can show from Eq. (29) that if we deal only with scalar perturbations (i.e., such that  $h_{00} = 2\phi$  and  $h_{ij} = 2\psi\delta_{ij}$ ) then  $\Psi_{ab} = 0$ . For the vector and tensor perturbations,  $\Psi_{ab}$  does not vanish but in the thin lens approximation its contribution corresponds to a boundary term (time dependent but identical for all light rays joining the source and the observer) which can thus be dropped.

Then, the amplification matrix, in the thin lens approximation, reduces to

$$\mathcal{A}_{ab} = I_{ab} - 4G \frac{\lambda_S - \lambda_L}{\lambda_S} \lambda_L \partial_a \partial_b \int \ln|\vec{x}_\perp - \vec{x}'_\perp| \Sigma(\vec{x}'_\perp) d^2 \vec{x}'_\perp \quad (35)$$

which can be rewritten, after the change of variables  $\vec{\theta}' = \vec{x}'_\perp / \lambda_S$ , as

$$\begin{aligned} \mathcal{A}_{ab}(\lambda_S) = & I_{ab} - 4G \frac{\lambda_S - \lambda_L}{\lambda_S} \partial_{\theta_1^a} \partial_{\theta_1^b} \\ & \times \int \ln|\vec{\theta}_1 - \vec{\theta}'| \lambda_L \Sigma(\vec{\theta}') d^2 \vec{\theta}'. \end{aligned} \quad (36)$$

Decomposing  $\Sigma(\vec{\theta})$  as  $\lambda_L \Sigma(\vec{\theta}) = \int \mu(s) \delta[\vec{\theta} - \vec{\theta}_{\text{string}}(s)] ds$ , where  $\vec{\theta}_{\text{string}}$  represents the locus of the string on the plane  $x_{\parallel} = x_{\parallel}(\lambda_L)$ , we get that Eq. (36) reduces to

$$\mathcal{A}_{ab}(\lambda_S) = I_{ab} - \partial_{\theta_1^a} \partial_{\theta_1^b} \varphi(\vec{\theta}_1)$$

with

$$\varphi(\vec{\theta}_1) \equiv 4G \frac{\lambda_S - \lambda_L}{\lambda_S} \int \ln|\vec{\theta}_1 - \vec{\theta}_{\text{string}}(s)| \mu(s) ds, \quad (37)$$

where  $\mu(s)$  is the projected total lineic energy density of the string (which mixes the effect of the lineic energy, the tension and the currents along the string if any) and  $\varphi$  is the effective projected potential.

When dealing with topological defects, there are different reasons why such an approximation may not hold. First the strings are extended and move with relativistic speed so that (i) they are *a priori* not confined in a plane  $\lambda_L \approx \text{constant}$  and (ii) one cannot assume that the distribution of matter of the lens is static so that the time dependence in the line-of-sight integration in Eq. (24) has to be taken into account. These issues will be addressed in Sec. IV B after a description of the general stress-energy tensor of strings (Sec. III).

## D. Comments

### 1. Gravitational potential and deflecting potential

As a first comment, let us stress that in general the deflecting potential  $\Phi$  is different from the Newtonian gravitational potential. For instance, a general perturbed spacetime has the general post-Newtonian metric

$$ds^2 = -(1 - 2\phi)dt^2 + 2A_i dx^i dt + [(1 + 2\psi)\delta_{ij} + 2\bar{E}_{ij}]dx^i dx^j, \quad (38)$$

where  $\phi$  and  $\psi$  are the Newtonian potentials,  $A_i$  and  $\bar{E}_{ij}$  are the vector (rotational) and tensor (gravitational waves) perturbations satisfying

$$\bar{E}_i^i = \partial_i \bar{E}^{ij} = \partial_i A^i = 0. \quad (39)$$

It follows that

$$\Phi = \phi + \psi + A_i \gamma^i + \bar{E}_{ij} \gamma^i \gamma^j, \quad (40)$$

where  $\gamma^i$  is the direction of observation. This includes effects from the rotation of the deflecting body and of gravitational waves. Indeed, in the case of pure scalar perturbations, we recover that

$$\Phi = 2\phi.$$

In the case of scalar perturbations, one can easily check that  $\Psi_{ab} = 0$  but topological defects also generate vector and tensor perturbations. In the thin lens approximation, the contribution of these two terms reduces to a boundary term that can be neglected but in the general case of extended object, one has to check that it is still the case for the vector and tensor modes.

### 2. Deflection angle

In a general spacetime, the deflection is not straightforward to define. This is, for instance, the case in a perturbed spacetime with perturbations on all scales (see, e.g., Refs. [35,36] for a discussion and a generalization of this concept). If the matter perturbation causing the lensing is localized in space then the metric perturbations generally die away and the spacetime is asymptotically unperturbed. In that case, one can compute the deflection angle simply by solving the

geodesic equation (3) at first order in the perturbations. For that purpose, we decompose the tangent vector to the geodesic  $g$  as

$$k_g^\mu = \bar{k}^\mu + \delta k^\mu. \quad (41)$$

$\bar{k}^\mu$  is the tangent vector of the light ray in the unperturbed Minkowski spacetime. Note that  $\bar{k}^\mu$  is different from the vector  $k^\mu$  defined in Eq. (2) which labels the geodesic of reference  $g_0$ . At first order in the perturbation, it is in fact possible to choose the unperturbed geodesic as reference since the displacement  $\xi$  is first order in the perturbation.

Since both  $\eta_{\mu\nu} \bar{k}^\mu \bar{k}^\nu = 0$  and  $g_{\mu\nu} k^\mu k^\nu = 0$ , we deduce that  $\bar{k}^\mu \delta k_\mu = 0$  at first order in the perturbations. At linear order, the geodesic equation (3) implies that

$$\frac{d}{d\lambda} \delta k^\alpha + \delta \Gamma_{\mu\nu}^\alpha \bar{k}^\mu \bar{k}^\nu = 0 \quad (42)$$

with  $\delta \Gamma_{\mu\nu}^\alpha \equiv \frac{1}{2} \eta^{\alpha\beta} (h_{\beta\mu,\nu} + h_{\beta\nu,\mu} - h_{\mu\nu,\beta})$ , so that

$$[\delta k^\alpha]_{\lambda_S}^0 = -\eta^{\alpha\nu} [h_{\mu\nu} \bar{k}^\mu]_{\lambda_S}^0 + \frac{1}{2} \eta^{\alpha\beta} \int_{\lambda_S}^0 h_{\mu\nu,\beta} \bar{k}^\mu \bar{k}^\nu d\lambda, \quad (43)$$

the integral being performed along the unperturbed geodesic. Forgetting the boundary term (which is a time dependent term but identical for all light rays joining the source and the observer), we can extract the variation of the photon energy measured by an observer with velocity  $u^\mu$ ,

$$\delta E = \int_{\lambda_S}^0 \partial_t \Phi[\vec{x}_\perp, x_\parallel(\lambda), t(\lambda)] d\lambda, \quad (44)$$

and the deflection  $\vec{\alpha}$  in the plane perpendicular to the line of sight:

$$\vec{\alpha} = \vec{\nabla}_\perp \int_{\lambda_S}^0 \Phi[\vec{x}_\perp, x_\parallel(\lambda), t(\lambda)] d\lambda. \quad (45)$$

The effect on the photon energy, and thus on its redshift, is nothing else but the well known Sachs-Wolfe effect [37].

Focusing on Eq. (45), since  $\Phi$  is evaluated along the photon geodesic  $t(\lambda) = t_0 - x_\parallel(\lambda)$ , we deduce that

$$[\partial_t + \partial_{x_\parallel}] \Phi[\vec{x}_\perp, x_\parallel(\lambda), t(\lambda)] = 0 \quad (46)$$

along the photon path. Hence, rewriting the three dimensional Laplacian as  $\Delta = \partial_{x_\parallel}^2 + \Delta_\perp$ , where  $\Delta_\perp$  is the two dimensional Laplacian and using the Einstein equations (19), we deduce that

$$\begin{aligned} \vec{\nabla}_\perp \cdot \vec{\alpha} &= -8\pi G \int_{\lambda_S}^0 \mathcal{F}[\vec{x}_\perp, x_\parallel(\lambda), t(\lambda)] d\lambda \\ &= -8\pi G \int_0^{t(\lambda_S) - t_0} \mathcal{F}[\vec{x}_\perp, x_\parallel(t), t] dt \end{aligned} \quad (47)$$



after choosing the parametrization  $\lambda = t_0 - t$  and where we have introduced  $\mathcal{F} \equiv \mathcal{F}_{\mu\nu} k^\mu k^\nu = T_{\mu\nu} k^\mu k^\nu$ . It follows that the 2-divergence of the deflection depends only on the projection of  $\mathcal{F}_{\mu\nu}$  onto the photon trajectory in between the source and the observer and thus vanishes on all directions which do not intersect the string worldsheet. Note that such a result holds for any relativistic and/or extended lens.

Now, in the thin lens approximation, one can relate  $\theta_S$  and  $\theta_I$  (see Fig. 1) by

$$\theta_S^a = \theta_I^a - \frac{\lambda_S - \lambda_L}{\lambda_S} \alpha^a. \quad (48)$$

The amplification matrix being given by  $\mathcal{A}_b^a = d\theta_S^a/d\theta_I^b$ , we obtain that

$$\mathcal{A}_{ab} = I_{ab} + \frac{\lambda_S - \lambda_L}{\lambda_S} \partial_{\theta^b} \partial_a \int_0^{\lambda_S} \Phi d\lambda. \quad (49)$$

Since the lens is localized in planes close to  $\lambda = \lambda_L$ , we have that  $\partial_{\theta^a} \approx \lambda_L \partial_a$  so that the former expression of the amplification matrix reduces to Eq. (35) once we use the expression (34) for the integrated potential. In both approaches, we find that the deflection angle is given by the usual expression (see, e.g., Ref. [44])

$$\vec{\alpha} = 4G\lambda_L \int \frac{\vec{\theta}^I - \vec{\theta}'}{|\vec{\theta}^I - \vec{\theta}'|^2} \Sigma(\theta') d^2 \vec{\theta}'$$

and we emphasize that defining the amplification matrix through the deflection angle implicitly assumes that we are in the thin lens approximation [as seen, for instance, in Eq. (48)].

### 3. Applicability to cosmology

It has probably not escaped a careful reader that we have restricted our calculations to perturbations around a Minkowski spacetime. The justification of such a choice is that the null geodesics of two conformal spacetimes are identical, so that lensing effects are the same. The only difference when considering an expanding Friedman-Lemaître universe will be the computation of the distances, i.e., of  $\lambda_S$  and  $\lambda_L$  in Eq. (36). Note also that the expansion of the universe affects the dynamics of the topological defects network (see, e.g., Ref. [38]) but this will not be relevant on time scales of order of the impact parameter which are small compared to the dynamical scales of the universe.

## III. DYNAMICS OF COSMIC STRINGS

The determination of the amplification matrix  $\mathcal{A}$  requires the knowledge of stress-energy tensor of the cosmic strings. In this section, we first present the definition of this tensor and derive the equation of motion of a string. We then focus on the particular case of a nonrotating cosmic loop.

### A. Equations of motion of the string

As shown by Carter [39], there is an elegant way to describe the dynamics of a ( $d < n$ )-brane embedded in a  $n$ -dimensional spacetime. In this section, we recall the main steps of this formalism necessary to obtain the dynamical equation of evolution of the string; details can be found in Ref. [39]. It requires the introduction of the induced metric on the string world sheet

$$f_{AB} \equiv g_{\mu\nu} x_{,A}^\mu x_{,B}^\nu, \quad (50)$$

where  $A, B, \dots$ , refers to coordinates on the world sheet and from which one can construct the fundamental tensor  $\bar{\eta}^{\mu\nu}$  and the orthogonal projector  $\perp^{\mu\nu}$  as

$$\bar{\eta}^{\mu\nu} \equiv f^{AB} x_{,A}^\mu x_{,B}^\nu, \quad \text{and} \quad \perp_\nu^\mu \equiv g_\nu^\mu - \bar{\eta}_\nu^\mu. \quad (51)$$

The covariant derivative  $\nabla$  defines a tangentially projected differentiation operator

$$\bar{\nabla}_\mu \equiv \bar{\eta}_\mu^\nu \nabla_\nu. \quad (52)$$

The second fundamental tensor is defined by

$$K_{\mu\nu}{}^\rho \equiv \bar{\eta}_\nu^\sigma \bar{\nabla}_\mu \bar{\eta}_\sigma^\rho, \quad (53)$$

and the condition that the world sheet is integrable, i.e., that all its elements mesh to form a well defined  $d$ -surface, is expressed by

$$K_{[\mu\nu]}{}^\rho = 0, \quad (54)$$

which is a *geometric identity* for the world sheet.

In the case of a string ( $d=2$ ), the Lagrangian density  $\hat{\mathcal{L}}$  can be expressed as

$$\hat{\mathcal{L}} = \frac{1}{\sqrt{-g}} \int \sqrt{f} d^2 \xi \bar{\mathcal{L}} \delta^{(4)}[x^\mu - x^\mu(\xi^A)], \quad (55)$$

where  $f$  is the determinant of the metric  $f_{AB}$  defined in Eq. (50).  $\hat{\mathcal{L}}$  is distributional and not confined to the string world sheet whereas  $\bar{\mathcal{L}}$  is locally regular but confined on the string world sheet. The string action can then be written either in terms of  $\hat{\mathcal{L}}$  or of  $\bar{\mathcal{L}}$  as

$$S_{\text{string}} = \int d^2 \xi \sqrt{f} \bar{\mathcal{L}} = \int d^4 x \sqrt{-g} \hat{\mathcal{L}}. \quad (56)$$

Now, making an infinitesimal variation  $\delta g_{\mu\nu}$  of the action (56) provides a definition of the “surface” stress energy tensor density  $\hat{T}^{\mu\nu}$  (confined and regular) and of the stress energy tensor density  $\hat{T}^{\mu\nu}$  (distributional and unconfined) by

$$2\delta S_{\text{string}} = \int d^2 \xi \sqrt{f} \hat{T}^{\mu\nu} \delta g_{\mu\nu} = \int d^4 x \sqrt{-g} \hat{T}^{\mu\nu} \delta g_{\mu\nu}.$$

These two stress-energy tensors are related by

$$\hat{T}^{\mu\nu} = \frac{1}{\sqrt{-g}} \int d^2\zeta \sqrt{f} \tilde{T}^{\mu\nu} \delta^{(4)}[x^\mu - x^\mu(\zeta^A)]. \quad (57)$$

The internal coordinate stress energy tensor  $\tilde{T}^{AB}$  has been projected onto a corresponding background stress energy tensor  $\tilde{T}^{\mu\nu}$  as in Eq. (51). One can then show that the general form of the *dynamical equation* of the string is

$$\bar{\nabla}_\mu \tilde{T}^{\mu\nu} = f^\nu, \quad (58)$$

$f^\nu$  being the force exerted on the string by any background field such as, e.g., an electromagnetic field. This dynamical equation (58) is equivalent to the more natural equation of conservation  $\nabla_\mu \hat{T}^{\mu\nu} = \hat{f}^\nu$  with  $\hat{f}^\nu$  related to  $f^\nu$  as in Eq. (57).

For a string of energy per unit length  $U$  and of tension  $T$ , the surface stress energy tensor density is of the form

$$\tilde{T}^{\mu\nu} = U u^\mu u^\nu - T v^\mu v^\nu, \quad (59)$$

where  $u^\mu$  and  $v^\mu$  are, respectively, a timelike ( $u^\mu u_\mu = -1$ ) and a spacelike ( $v^\mu v_\mu = +1$ ) unit vector tangent to the string world sheet (i.e.,  $\perp_\nu u^\nu = \perp_\nu v^\nu = 0$ ) so that  $\bar{\eta}^{\mu\nu} = -u^\mu u^\nu + v^\mu v^\nu$ . The dynamical equation governing the evolution of the string is given by the tangential projection of Eq. (58) which, in the free case we are considering, leads to

$$\eta^\rho_\nu \bar{\nabla}_\mu \tilde{T}^{\mu\nu} = 0. \quad (60)$$

This equation of evolution (60) can then be solved once we are given an equation of state, i.e.,  $U(T)$ . Such equations are provided once the microscopic structure of the string is described. The most well known are the Goto-Nambu strings [40] ( $U=T=\text{constant}$ ) and the Nielsen-Olesen strings [41] ( $U+T=\text{constant}$ ) and some have been obtained for superconducting strings [42].

### B. Application to a nonrotating cosmic string loop

In the case of a nonrotating circular loop of radius  $R$ , we work in cylindrical coordinates  $(t, r, \theta, z)$  and assume that it is lying in the plane  $z = z_s$ . Parametrizing the loop world sheet as

$$t_{\text{loop}} = t, \quad \vec{r}_{\text{loop}} \equiv \vec{r}_\perp = R(t)(\cos \theta, \sin \theta), \quad x_3 \equiv z_{\text{loop}} - z_s = 0, \quad (61)$$

one can show that the unit spacelike vector tangent to the string world sheet is  $v^\mu = \theta^\mu$  and we have

$$u_\mu = \gamma \delta_\mu^t + \gamma \dot{R} \delta_\mu^r, \quad \theta_\mu = R \delta_\mu^\theta, \quad (62)$$

with  $\gamma \equiv (1 - \dot{R}^2)^{-1/2}$  being the Lorentz factor associated with the radial contraction and expansion of the string. They satisfy  $\perp_\nu u^\nu = \perp_\nu v^\nu = 0$ . From Eqs. (59) and (57), the stress-energy tensor entering the Einstein equations (19) is given by

$$T^{\mu\nu}(\vec{x}, t) = \begin{pmatrix} \gamma^2 U & \gamma^2 \dot{R} U & 0 & 0 \\ \gamma^2 \dot{R} U & \gamma^2 \dot{R}^2 U & 0 & 0 \\ 0 & 0 & -R^2 T & 0 \\ 0 & 0 & 0 & 0 \end{pmatrix} \times \delta(z - z_s) \delta(r - R). \quad (63)$$

We now need to write the dynamical evolution equation (60) to get the evolution of the radius of the loop as a function of time. Using that  $\bar{\eta}_{\mu\nu} = -u_\mu u_\nu + \theta_\mu \theta_\nu$  and the expression (59) of the stress-energy tensor of the string, Eq. (60) can be rewritten as

$$(-u_\mu u^\nu + \theta_\mu \theta^\nu) \nabla_\nu (U u^\mu u^\rho - T \theta^\mu \theta^\rho) = 0, \quad (64)$$

which reduces to

$$\frac{d}{dt}(\gamma U R) = 0, \quad (65)$$

$$\frac{d^2}{dt^2} R = -\frac{1}{\gamma^2 R} \frac{T}{U}. \quad (66)$$

This system of equations for  $(U, T, R)$  is not closed and can be solved when one specifies an equation of state  $U(T)$ . Equation (65) shows that the total energy  $\gamma R U$  of the loop is a constant of motion. Note that we have not used the identity (54) which is identically satisfied in our present example.

## IV. LENSING BY A COSMIC STRING

### A. A first example

As a first application, let us consider a static straight cosmic string lying along the axis  $x_2$  in a plane perpendicular to the line of sight (direction  $x_3$  on Fig. 4 with  $\varphi=0$ ) so that

$$\mathcal{F}_{\mu\nu} = \frac{1}{2} \begin{pmatrix} U-T & & & \\ & U+T & & \\ & & U-T & \\ & & & U+T \end{pmatrix} \delta(\lambda_L \theta_1) \times \delta[x_\parallel - x_\parallel(\lambda_L)], \quad (67)$$

with  $U$  and  $T$  depending on  $x_2 = \lambda_L \theta_2$  only. Since  $\mathcal{F} = U(x_2) \delta(x_1) \delta[x_\parallel - x_\parallel(\lambda_L)]$ , the first integral of Eq. (28), after integration over  $x'_1$ , reduces to

$$\mathcal{A}_{ab} = I_{ab} + 2 \frac{G}{\lambda_S} \int U(x'_2) dx'_2 \partial_{ab} J[(x_2 - x'_2)^2 + x_1^2]$$

with

$$J[(x_2 - x'_2)^2 + x_1^2] = \int_0^{\lambda_S} \frac{\lambda(\lambda_S - \lambda)}{\sqrt{(x_2 - x'_2)^2 + x_1^2 + (\lambda - \lambda_L)^2}} d\lambda,$$

where we have chosen a parametrization such that  $x_\parallel(\lambda) = \lambda$ . This latter integral can be computed and gives

$$\begin{aligned}
 J(A) = & \frac{1}{2}(\lambda_S - 3\lambda_L)\sqrt{A^2 + (\lambda_S - \lambda_L)^2} \\
 & - \left(\lambda_S - \frac{3}{2}\lambda_L\right)\sqrt{A^2 + \lambda_L^2} \\
 & + \left(\lambda_S\lambda_L - \lambda_L^2 + \frac{1}{2}A^2\right) \\
 & \times \ln \frac{\lambda_S - \lambda_L + \sqrt{A^2 + (\lambda_S - \lambda_L)^2}}{-\lambda_L + \sqrt{A^2 + \lambda_L^2}}
 \end{aligned}$$

with  $A \equiv \sqrt{(x_2 - x'_2)^2 + x_1^2}$ . It follows that the amplification matrix is given by

$$\begin{aligned}
 \mathcal{A}_{ab} = & I_{ab} + 2\frac{G}{\lambda_S} \int U(x'_2) dx'_2 \\
 & \times \left( \frac{J'(A)}{A} \delta_{ab} + (x_a - x'_a)(x_b - x'_b) \left[ \frac{J''(A)}{A^2} - \frac{J'(A)}{A^3} \right] \right),
 \end{aligned} \tag{68}$$

where  $J' \equiv dJ/dA$  and  $x'_1 = 0$ . We can perform a change of variable from  $x'_2$  to  $A$ . For that purpose we need to cut the integral over  $x'_2$  in two pieces, the first from  $-\infty$  to  $x_2$  where  $x'_2 = x_2 - \sqrt{A^2 - x_1^2}$  and the second from  $x_2$  to  $+\infty$  where  $x'_2 = x_2 + \sqrt{A^2 - x_1^2}$ . We thus obtain that the coefficients of the amplification matrix are given by

$$\begin{aligned}
 \mathcal{A}_{11} = & 1 + \frac{2G}{\lambda_S} \int_{|x_1|}^{\infty} [U(x_2 - \sqrt{A^2 - x_1^2}) + U(x_2 + \sqrt{A^2 - x_1^2})] \\
 & \times \left( \frac{J'}{A} + x_1^2 \left[ \frac{J''}{A^2} - \frac{J'}{A^3} \right] \right) \frac{AdA}{\sqrt{A^2 - x_1^2}}, \\
 \mathcal{A}_{22} = & 1 + \frac{2G}{\lambda_S} \int_{|x_1|}^{\infty} [U(x_2 - \sqrt{A^2 - x_1^2}) + U(x_2 + \sqrt{A^2 - x_1^2})] \\
 & \times \left( \frac{J'}{A} + (A^2 - x_1^2) \left[ \frac{J''}{A^2} - \frac{J'}{A^3} \right] \right) \frac{AdA}{\sqrt{A^2 - x_1^2}}, \\
 \mathcal{A}_{12} = & \frac{2G}{\lambda_S} \int_{|x_1|}^{\infty} [U(x_2 - \sqrt{A^2 - x_1^2}) - U(x_2 + \sqrt{A^2 - x_1^2})] \\
 & \times x_1 \left[ \frac{J''}{A^2} - \frac{J'}{A^3} \right] AdA.
 \end{aligned}$$

This gives the exact expression of the components of the amplification matrix and indeed this result depends on the density  $U$  along the string.

Now, let us try to estimate the dominant term in the integral of expression (68) when we are looking close to the string (i.e., when  $x_1, x_2 \ll \lambda_S - \lambda_L, \lambda_L$ ). For that purpose we

assume that  $\lambda_S - \lambda_L \sim \lambda_L$  and set  $\lambda \equiv \lambda_S - \lambda_L \sim \lambda_L$ . We first note that  $J(A)$  behaves, in the two following regimes, as

$$J(A) \simeq \begin{cases} -(\lambda_S - \lambda_L)\lambda_L \ln(A^2), & A/\lambda^2 \ll 1, \\ \frac{\lambda_S^3}{6A}, & A/\lambda^2 \gg 1, \end{cases}$$

which ensures that, as long as  $x_1 \neq 0$ , all the integrals over  $A$  converge. Now when we are looking closer and closer to the string (i.e.,  $x_1 \rightarrow 0$ ) the integrals (as functions of  $x_1$ ) diverge (as  $A^{-2}$  for  $\mathcal{A}_{11}$  and  $\mathcal{A}_{22}$  and as  $x_1 A^{-3}$  for  $\mathcal{A}_{12}$ ). This indicates that the integrals are dominated by their value in  $A \sim |x_1|$  (in a way  $|x_1|$  acts as a cut off regularizing the integrals) for which it is justified to approximate  $J(A)$  by a logarithm and thus

$$\mathcal{A}_{ab} \sim I_{ab} - 4G \frac{\lambda_S - \lambda_L}{\lambda_S} \partial_{\theta^a} \partial_{\theta^b} \int \ln |\vec{\theta}' - \vec{\theta}| U(\theta'_2) d\theta'_2. \tag{69}$$

Indeed, this is not a proof but only a Heuristic argument. The validity of this argument depends on the properties of  $U$ ; in the particular case where  $U$  is constant, this approximate gives the general result of the deflection by a straight cosmic string [19–21] and one can thus think that this is a good approximation when the large scales fluctuations are small enough to ensure the convergence of the integrals in Eq. (68) at large distance (i.e., when  $A \rightarrow \infty$ ). Note also that for such an infinite string lying in a plane perpendicular to the line of sight we recover the general form (37) of the deformation matrix in the thin lens approximation. In the following, we investigate more general results concerning the deformation fields by a cosmic string which do not assume that we are in the thin lens regime.

## B. General results

In the general case, the source term generated by a cosmic string will be localized on the string world sheet so that [see Eq. (59)]

$$\mathcal{F}(\vec{x}, t) = \int d\zeta \tilde{\mathcal{F}}(\vec{x}, t) \delta(\vec{x} - \vec{r}(\zeta, t)), \tag{70}$$

where  $(t, \vec{r}(\zeta, t))$  is a parametrization of the string world sheet,  $\vec{r}(\zeta, t)$  represents the locus of the string on each constant time hypersurface, and  $\tilde{\mathcal{F}}$  is the energy density per unit length [note that we have chosen a parametrization such that  $t$  is both the coordinate time and an intrinsic coordinate of the string world sheet which implies that we have a one-dimensional integration on the spatial internal coordinate  $\zeta$  and not a two-dimensional integration as in Eq. (59)]. Inserting this decomposition in Eq. (21), we deduce that the deflecting potential (27) is given, after integration over space, by



$$\Phi(\vec{x}, t) = 2G \int \frac{dt' d\zeta}{|\vec{x} - \vec{r}(\zeta, t')|} \tilde{\mathcal{F}}[\vec{r}(\zeta, t'), t'] \times \delta(t' - t + |\vec{x} - \vec{r}(\zeta, t')|). \quad (71)$$

Following Ref. [43], the integration over  $t'$  can be performed by introducing  $t_{\text{string}}(\vec{x}, \zeta, t)$  solution of

$$t - t_{\text{string}}(\vec{x}, \zeta, t) = |\vec{x} - \vec{r}(\zeta, t_{\text{string}}(\vec{x}, \zeta, t))| \quad (72)$$

$$\Phi(\vec{x}, t) = 2G \int \frac{\tilde{\mathcal{F}}[\vec{r}(\zeta, t_{\text{string}}(\vec{x}, \zeta, t)), t_{\text{string}}(\vec{x}, \zeta, t)]}{|\vec{x} - \vec{r}(\zeta, t_{\text{string}}(\vec{x}, \zeta, t))| - \partial_t \vec{r}(\zeta, t_{\text{string}}(\vec{x}, \zeta, t)) \cdot [\vec{x} - \vec{r}(\zeta, t_{\text{string}}(\vec{x}, \zeta, t))]} d\zeta. \quad (73)$$

$\Phi$  on the point  $(\vec{x}, t)$  is then given by the projection of the string energy on the past light cone of this point, i.e., on the curve  $\{\vec{r}(\zeta, t_{\text{string}}(\vec{x}, \zeta, t)), t_{\text{string}}(\vec{x}, \zeta, t)\}$  which is the intersection of the string world sheet with the past light cone of the event  $(\vec{x}, t)$  (see Fig. 2).

Now, focusing on  $\kappa$ , the deformation matrix is then given by Eqs. (28) and (29) with the deflecting potential  $\Phi$  given by Eq. (73) and, proceeding as for the deflection angle, one can easily sort out that

$$\begin{aligned} \delta^{ab} \mathcal{D}_{ab}^{(1)} &= \int_0^{\lambda_S} \lambda (\lambda_S - \lambda) \Delta_{\perp} \Phi(\vec{x}_{\perp}, x_{\parallel}(\lambda), t(\lambda)) d\lambda \\ &\quad + \int_0^{\lambda_S} \lambda (\lambda_S - \lambda) \delta^{ab} \Psi_{ab} d\lambda \\ &= \int_0^{\lambda_S} \lambda (\lambda_S - \lambda) [(\partial_t^2 + \partial_{\parallel}^2) \Phi(\vec{x}_{\perp}, x_{\parallel}(\lambda), t(\lambda)) \\ &\quad - 8\pi G \mathcal{F}(\vec{x}_{\perp}, x_{\parallel}(\lambda), t(\lambda))] d\lambda \end{aligned}$$

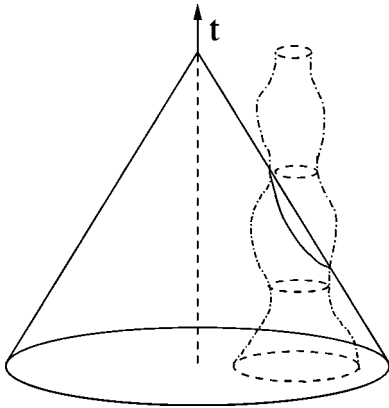


FIG. 2. The intersection of the loop world sheet and the past light cone of the event  $(\vec{x}, t)$ . The dash circles represent the loop in different constant time hypersurfaces and the dash-dot lines the loop world sheet.

so that

$$\begin{aligned} &\delta(t' - t + |\vec{x} - \vec{r}(\zeta, t')|) \\ &= \frac{|\vec{x} - \vec{r}(\zeta, t')|}{|\vec{x} - \vec{r}(\zeta, t')| - \partial_t \vec{r}(\zeta, t') \cdot (\vec{x} - \vec{r}(\zeta, t'))} \delta(t' - t_{\text{string}}) \end{aligned}$$

from which we deduce that

$$+ \int_0^{\lambda_S} \lambda (\lambda_S - \lambda) \delta^{ab} \Psi_{ab} d\lambda. \quad (74)$$

The first term of the first integral vanishes when evaluated on the photon geodesic so that the contribution of the first integral to the convergence  $\kappa$  defined in Eq. (15) reduces to

$$\begin{aligned} \kappa(\vec{x}_{\perp}, t_0) &= 4\pi G \int_0^{\lambda_S} \frac{\lambda (\lambda_S - \lambda)}{\lambda_S} \mathcal{F}(\vec{x}_{\perp}, x_{\parallel}(\lambda), t(\lambda)) d\lambda \\ &= 4\pi G \int_{t_{\text{emission}}}^{t_0} \frac{(t - t_{\text{emission}})(t_0 - t)}{t_0 - t_{\text{emission}}} \mathcal{F}(\vec{x}_{\perp}, x_{\parallel}(t), t) dt, \end{aligned} \quad (75)$$

where we recall that  $t_0 \equiv t(\lambda = 0)$  is the time of reception and where  $t_{\text{emission}} \equiv t(\lambda_S)$  is the time of emission. The contribution of the second integral of Eq. (74) vanishes since (i)  $\Psi_{ab} \delta^{ab} = 0$  both for scalar perturbations [ $\phi$  and  $\psi$  in Eq. (38)] and for vector perturbations [ $A_i$  in Eq. (38)] and (ii) for tensor modes [ $\bar{E}_{ij}$  in Eq. (38)]  $\Psi_{ab} \delta^{ab} \propto (d/d\lambda)[(\partial_t + \partial_{\parallel})(\bar{E}_1^1 + \bar{E}_2^2)] = 0$  when evaluated on the photon trajectory. We conclude that the convergence  $\kappa$  is given by Eq. (75). It is then given by the distribution of matter evaluated on the photon trajectory, up to a geometrical factor. The lensing by a cosmic string is thus equivalent to the lensing by a linear distribution of matter. *As a consequence*,  $\kappa = 0$  everywhere but on directions such that the observer past light cone intersects the string worldsheet; this result, valid whatever the equation of state, is one of the main results of this article. It holds for any relativistic lens and does not rely on the thin lens approximation.

For instance, if the string is lying in a plane perpendicular to the line of sight then Eq. (75) reduces to

$$\kappa(\vec{x}_{\perp}, t_0) = 4\pi G \frac{\lambda_S - \lambda_L}{\lambda_S} \lambda_L \Sigma(\vec{x}_{\perp}, x_{\parallel}(\lambda_L), t(\lambda_L)) \propto \nabla_{\perp} \cdot \vec{\alpha}. \quad (76)$$

With this form, again we see that  $\kappa=0$  everywhere but on directions intersecting the string world sheet.

Note that the derivation of Eq. (75) relies strongly on the fact that we took the trace of the deformation matrix in Eq. (74). Therefore, a similar expression to Eq. (75) cannot be obtained for the other components of the amplification matrix and one has to rely on Eq. (73).

It also has to be noted that the expression of the amplification matrix in Eq. (49) (which relies on the thin lens approximation) together with the general result (75) implies that the phenomenological description of  $\mathcal{A}_b^a$  in Eq. (37) is very general. It holds for any string dynamics provided the extension of the string is small enough for the thin lens approximation to hold. Different aspects of these results are illustrated in the next paragraphs. A more elaborate phenomenological investigation based on Eq. (37) is proposed in Ref. [28].

### C. Lensing by a nonrotating cosmic string loop perpendicular to the line of sight

We now consider as an application the case of a nonrotating circular loop oscillating in a plane perpendicular to the line of sight. Its dynamics is described by the set of equations (65),(66) and from its parametrization (61) we deduce that

$$\mathcal{F}(\vec{x}, t) = \int_0^{2\pi} R(t) \gamma(t) U(t) \delta(x_3) \delta(\vec{x}_\perp - \vec{r}_\perp) d\theta. \quad (77)$$

The deflecting potential (27) integrated along the line of sight is then given by

$$\begin{aligned} I[\Phi] &\equiv \int_0^{\lambda_S} \Phi[\vec{x}(\lambda), t(\lambda)] d\lambda \\ &= 2G \int_{-x_L}^{x_S - x_L} dx_3 \int_0^{2\pi} d\theta \int_{R^2} d^2\vec{x}'_\perp \int_{-\infty}^{+\infty} dt' \gamma R U \frac{\delta[t' + x_3 - \tau_0 + \sqrt{(\vec{x}_\perp - \vec{x}'_\perp)^2 + x_3^2}]}{\sqrt{(\vec{x}_\perp - \vec{x}'_\perp)^2 + x_3^2}} \delta(\vec{x}'_\perp - \vec{r}_\perp(t', \theta)), \end{aligned} \quad (78)$$

where we have parametrized the geodesic as  $t = \tau_0 - x_3$  with  $\tau_0 \equiv t_0 - x_L$ . Now, defining the new variable  $z$  as

$$z \equiv x_3 + \sqrt{(\vec{x}_\perp - \vec{x}'_\perp)^2 + x_3^2} \quad (79)$$

which satisfies

$$\frac{dz}{z} = \frac{dx_3}{\sqrt{(\vec{x}_\perp - \vec{x}'_\perp)^2 + x_3^2}}. \quad (80)$$

The integrated potential (78) reduces to

$$\begin{aligned} I[\Phi] &= 2G \int_0^{2\pi} d\theta \int_{R^2} d^2\vec{x}'_\perp \int_A \frac{dz}{z} \int_{-\infty}^{+\infty} dt' \gamma R U \\ &\quad \times \delta(t' + z - \tau_0) \delta(\vec{x}'_\perp - \vec{r}_\perp(t', \theta)), \end{aligned} \quad (81)$$

where the limits of integration are

$$A = -x_L + \sqrt{(\vec{x}_\perp - \vec{x}'_\perp)^2 + x_L^2} \approx \frac{1}{2} \frac{(\vec{x}_\perp - \vec{x}'_\perp)^2}{x_L}, \quad (82)$$

$$B = x_S - x_L + \sqrt{(\vec{x}_\perp - \vec{x}'_\perp)^2 + (x_S - x_L)^2} \approx 2(x_S - x_L). \quad (83)$$

The approximate values of  $A$  and  $B$  are obtained at lowest order when we consider zones close to the string in comparison with the distance string observer and string source.

After integration over  $t'$  and using the loop equation of motion (65),(66) which state that  $\gamma R U$  is constant, we get that

$$I[\Phi] = 2G \gamma R U J(\vec{x}_\perp, t_0), \quad (84)$$

where  $J(\vec{x}_\perp, t_0)$  is a dimensionless geometrical integral given by

$$\begin{aligned} J(\vec{x}_\perp, t_0) &= \int_0^{2\pi} d\theta \int_{R^2} d^2\vec{x}'_\perp \int_{(1/2)[(\vec{x}_\perp - \vec{x}'_\perp)^2/x_L]}^{2(x_S - x_L)} \frac{dz}{z} \\ &\quad \times \delta(\vec{x}'_\perp - \vec{r}_\perp(-z + \tau_0, \theta)). \end{aligned} \quad (85)$$

This integral can be rewritten as

$$\begin{aligned} J(\vec{x}_\perp, t_0) &= \int_0^{2(x_S - x_L)} \frac{dz}{z} \int_0^{2\pi} d\theta \int_{|\vec{x}_\perp - \vec{x}'_\perp|^2 < 2x_L z} d^2\vec{x}'_\perp \\ &\quad \times \delta(\vec{x}'_\perp - \vec{r}_\perp(-z + \tau_0, \theta)). \end{aligned} \quad (86)$$

We deduce that, at  $z$  constant, the integral over  $\vec{x}'_\perp$  reduces to the computation of the angle  $\beta$  (see Fig. 3) of string within the disk of radius  $\sqrt{2x_L z}$  which can be computed as follows.

Setting  $u \equiv \sqrt{2x_L z}$  and  $h \equiv OH$ , we deduce from

$$u = u_1 + u_2, \quad u_1^2 + h^2 = \vec{x}_\perp^2, \quad u_2^2 + h^2 = R^2, \quad (87)$$

where  $u_1 \equiv CH$  and  $u_2 \equiv HD$  on Fig. 3 and  $R$  now stands for  $R(t = \tau_0)$ , that

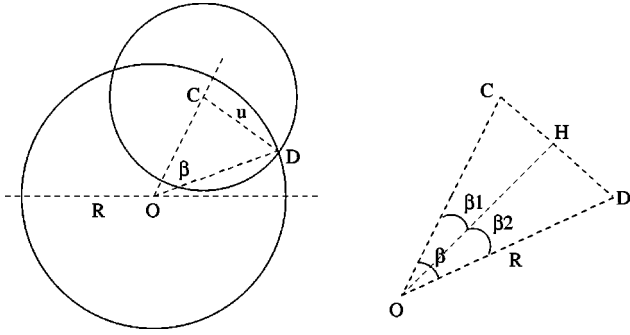


FIG. 3. Integration over the disk of radius  $u \equiv \sqrt{2x_L z}$  around the point  $C \equiv \vec{x}_\perp$ .

$$u_1 = \frac{\vec{x}_\perp^2 - R^2 + u^2}{2u}, \quad u_2 = \frac{-\vec{x}_\perp^2 + R^2 + u^2}{2u} \quad (88)$$

and thus that

$$\cos \beta = \frac{\vec{x}_\perp^2 + R^2 - u^2}{2|\vec{x}_\perp|R}. \quad (89)$$

The integral over  $\theta$  and  $\vec{x}'_\perp$  obviously vanishes if  $u < ||\vec{x}_\perp| - R|$ , reduces to  $2\pi$  when  $u > |\vec{x}_\perp| + R$  and gives  $2\beta(u)$  otherwise. Then, after splitting the integral over  $u$  in Eq. (86) in three pieces ( $[0, ||\vec{x}_\perp| - R|]$ ,  $[||\vec{x}_\perp| - R|, |\vec{x}_\perp| + R]$ , and  $[|\vec{x}_\perp| + R, 2\sqrt{x_L(x_S - x_L)}]$ ) we get

$$J(\vec{x}_\perp, t_0) = \int_{||\vec{x}_\perp| - R|}^{|\vec{x}_\perp| + R} 2\beta(u) \frac{du}{u} + 2\pi \int_{|\vec{x}_\perp| + R}^{2\sqrt{x_L(x_S - x_L)}} \frac{du}{u}, \quad (90)$$

with  $\beta$  given by Eq. (89). We can compute this integral in the two following regimes.

(1) If  $|\vec{x}_\perp| < R(\tau_0)$ , Eq. (90) can be rewritten as

$$J = 2|\vec{x}_\perp|R \int_{-1}^1 \frac{\text{Arccos } v}{|\vec{x}_\perp|^2 + R^2 - 2|\vec{x}_\perp|Rv} dv + 2\pi \ln \left[ \frac{2\sqrt{x_L(x_S - x_L)}}{|\vec{x}_\perp| + R} \right] \quad (91)$$

which can be computed to give

$$J = C_1, \quad (92)$$

where  $C_1$  is a constant depending on  $x_L$ ,  $x_S$ , and  $R(\tau_0)$ . Then, there is no deflection of a light ray passing inside a large loop, as first pointed out in Ref. [18] and as expected from the Gauss theorem.

(2) If  $|\vec{x}_\perp| > R(\tau_0)$ , Eq. (91) now gives after integration

$$J = C_1 - 2\pi \ln \frac{|\vec{x}_\perp|}{R} \quad (93)$$

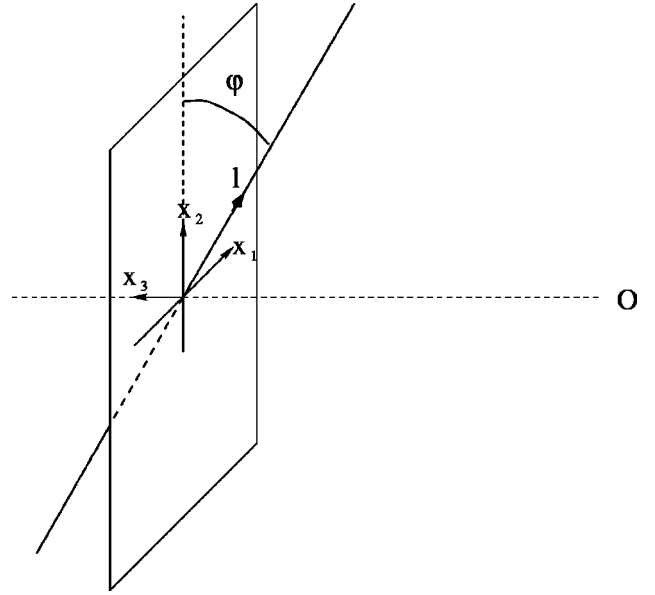


FIG. 4. Parametrization of a static straight tilted cosmic string.

and we conclude that a small loop perpendicular to the line of sight acts as a point mass  $M = 2\pi\gamma RU$  whatever its equation of state. We checked that this is also valid for a tilted circular loop and it is natural to expect that the fact that a loop acts as a point mass at a distance larger than its characteristic size is valid whatever the geometry of the loop.

One can also check from Eqs. (92),(93) that  $\Delta_\perp J(\vec{x}_\perp, t_0) = 0$  if  $\vec{x}_\perp \neq R(\tau_0)$ . Since  $\kappa \propto \Delta_\perp J$ , we recover the result from Eq. (75) that the convergence vanishes if  $\vec{x}_\perp \neq \vec{r}_\perp$ .

#### D. Tilted static straight cosmic string

To finish, let us consider a tilted static straight cosmic string aligned along an axis making an angle  $\varphi$  with the direction  $x_2$  (see Fig. 4) and for which, from Eq. (67),

$$\mathcal{F} = \int [U(l) - T(l) \sin^2 \varphi] dl \delta(\vec{x} - \vec{r}(l)), \quad (94)$$

where  $\vec{r}(l)$  is a parametrization of the string. If we choose  $l$  such that

$$\vec{r}(l): \quad r_1 = 0, \quad r_2 = l \cos \varphi, \quad r_3 = x_\parallel(\lambda_L) - l \sin \varphi, \quad (95)$$

the deflecting potential (73) is given by

$$\Phi(\vec{x}) = 2G \int \frac{dl}{|\vec{x} - \vec{r}(l)|} [U - T \sin^2 \varphi](l). \quad (96)$$

We recall that  $\vec{x} = (x_1, x_2, x_\parallel)$ . After performing the change of variable  $x_3 \equiv x_\parallel - x_L$  [see Fig. 4,  $x_L \equiv x_\parallel(\lambda_L)$ ], the deflecting potential (96) takes the form

$$\Phi(x_1, x_2, x_3) = 2G \int \frac{[U - T \sin^2 \varphi](l) dl}{\sqrt{x_1^2 + (x_2 - l \cos \varphi)^2 + (x_3 + l \sin \varphi)^2}}.$$

When  $U$  and  $T$  are constant, it can be integrated to give

$$\Phi(\vec{x}) = 2G[U - T \sin^2 \varphi] \{C_\infty - \ln[\vec{x}^2 - (x_2 \cos \varphi + x_3 \sin \varphi)^2]\}, \quad (97)$$

where  $C_\infty$  is an infinite constant. The infinite constant  $C_\infty$  can then be forgotten because only the derivatives of  $\Phi$  enters the computation of the deflection angle and of the amplification matrix which are the observable quantities. The deflection angle is then given by

$$\vec{\alpha} = -\nabla_\perp \int_{-x_L}^{x_S - x_L} \Phi(x_1, x_2, x_3) dx_3. \quad (98)$$

After integration over  $x_3$ , we get

$$\begin{aligned} \alpha_1 &= \frac{4G[U - T \sin^2 \varphi]}{\cos \varphi} \\ &\times \left[ \arctan\left(\frac{x_2 \sin \varphi + x_3 \cos \varphi}{x_1}\right) \right]_{x_3 = -x_L}^{x_3 = x_S - x_L}, \\ \alpha_2 &= 4G[U - T \sin^2 \varphi] \tan \varphi \\ &\times [\ln \sqrt{x_1^2 + (x_2 \sin \varphi + x_3 \cos \varphi)^2}]_{x_3 = -x_L}^{x_3 = x_S - x_L}. \end{aligned} \quad (99)$$

Note that we have integrated from the source ( $x_\parallel = x_S$ , i.e.,  $x_3 = x_S - x_L$ ) to the observer ( $x_\parallel = 0$ , i.e.,  $x_3 = -x_L$ ). In the limit where  $(x_S - x_L)|\cos \varphi|$  and  $x_L|\cos \varphi|$  are much larger than  $|x_1|$  and  $|x_2 \sin \varphi|$ , we get

$$\begin{aligned} \alpha_1 &\simeq 4\pi G[U \cos \varphi + (U - T) \sin \varphi \tan \varphi], \\ \alpha_2 &\simeq 4GU \tan \varphi \ln \frac{x_S - x_L}{x_L}. \end{aligned} \quad (100)$$

This has to be compared with the standard result for a Goto-Nambu string for which  $\alpha = 4\pi G U \cos \varphi$  [4,15,19,20]. Now, as pointed out by Peter [21] in the case of a string perpendicular to the line of sight, there are two origins to the deflection: the deficit angle (term proportional to  $U + T$ ) and a contribution from the curvature (proportional to  $U - T$ ). One can understand such a result by decomposing the stress-energy tensor (67) as  $2\mathcal{F}_{\mu\nu} = 2U \times \text{diag}(0,1,0,1) + (U - T) \times \text{diag}(1,-1,1,-1)$ , i.e., as the superposition of a Goto-Nambu string and a linear distribution of nonrelativistic matter of density  $\rho \equiv U - T$  per unit length. Then it is straightforward to see that the bending angle of the second contribution depends only on the projected mass per unit length and thus becomes larger by a factor  $1/\cos \varphi$  as found in Eq. (100). A consequence of this result is that, for general cosmic strings not perpendicular to the line of sight, one expects to have larger deflection than for a Goto-Nambu string.

In this case, the accuracy of the thin lens approximation can be investigated. For that purpose, we remind the reader that the shear is given by

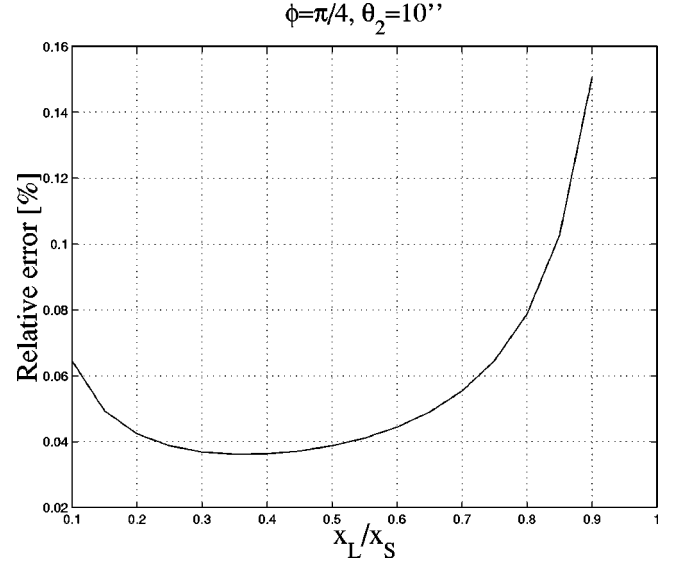


FIG. 5. Relative error on the geometric factor with respect to the thin lens result for a string with a tilt  $\varphi = \pi/4$  on a field  $\theta_2 = 10''$ . The relative error scales as  $(\theta_2/10'') \times \tan \varphi$ .

$$\begin{aligned} \left( \frac{\gamma_1}{\gamma_2} \right) &= 2G \int_{-x_L}^{x_S - x_L} \frac{(x_L + x_3)(x_S - x_L - x_3)}{x_S} \left( \frac{1}{2} [\partial_2^2 - \partial_1^2] \right) \\ &\times \int_{-\infty}^{\infty} \frac{[U(l) - T(l) \sin^2 \varphi] dl}{\sqrt{x_1^2 + (x_2 - l \cos \varphi)^2 + (x_3 - l \sin \varphi)^2}}. \end{aligned} \quad (101)$$

Because of the derivatives with respect to  $x_1$  and  $x_2$ , it is easy to see that the integral over  $l$  is peaked around  $x_3 \sim l \sin \varphi \sim x_2 \tan \varphi$ . Thus, on a field of width  $x_2 = x_S \theta_2$ , the variation of geometric factor is bounded by

$$\begin{aligned} \frac{\delta |(x_L - x_3)(x_S - x_L - x_3)|}{x_L(x_S - x_L)} &\simeq \frac{\left(1 + 2\frac{x_L}{x_S}\right)}{x_L/x_S(1 - x_L/x_S)} |\tan \varphi| \theta_2 \\ &< \frac{3}{x_L/x_S(1 - x_L/x_S)} |\tan \varphi| \theta_2, \end{aligned}$$

from which we deduce that since  $\theta_2 \ll 1$ , the thin lens approximation is still very good for tilted string with a tilt not larger than  $\varphi = \pi/4$  say (see Fig. 5 for a numerical estimation of the relative error).

## E. Discussion

In this section, we have shown that the deflecting potential of any extended lens with relativistic motion is obtained by considering the projected energy density on the photon past the light cone. This implies, in the case of cosmic strings, that the convergence  $\kappa$  vanishes everywhere but on the string projection.

We then studied the case of a loop oscillating in a plane perpendicular to the line of sight and show that the equation

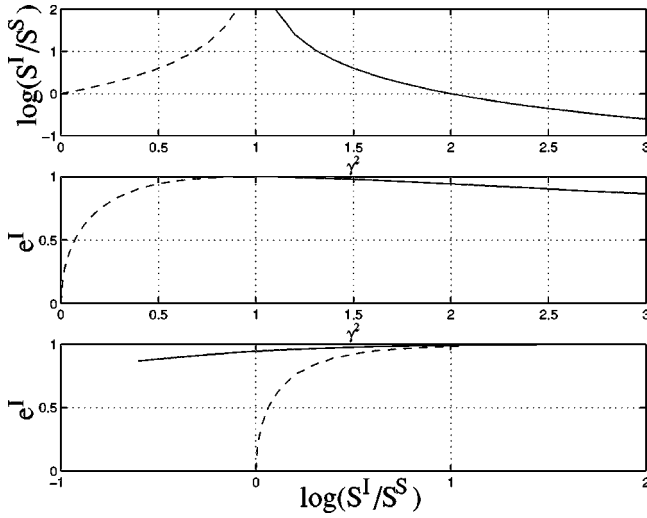


FIG. 6. The variation of  $S^I/S^S$  (top panel),  $e^I$  (middle panel) in function of  $\gamma$  and the set of the images (lower panel) for a circular source ( $e^S=0$ ) of surface  $S^S$ . The two branches represent, respectively, deformations such that  $\gamma < 1$  (dashed line) and  $\gamma > 1$  (solid line).

of motion of the loop can be used to integrate the deflecting potential. We found that a photon propagating inside such a circular loop was not deflected and those propagating outside were deflected as if the loop was a point mass object. This generalizes the result by de Laix and Vachaspati [24] to strings with any equation of state and shows how the equation of motion of the loop enables to factorize the integrated deflecting potential. This lets us conjecture that this result will be valid whatever the geometry of the loop, the geometric factor  $J$  being different for each loop geometry. We finished by discussing the case of static tilted cosmic strings to emphasize that, for non-Goto-Nambu strings, there can be larger deflections and we also discussed on this example the validity of the thin lens approximation for strings.

## V. PHENOMENOLOGY OF A DEFORMATION FIELD WITH $\kappa=0$

As seen in the previous section, we expect the deformation field of a cosmic string to be such that  $\kappa=0$ . Indeed, in

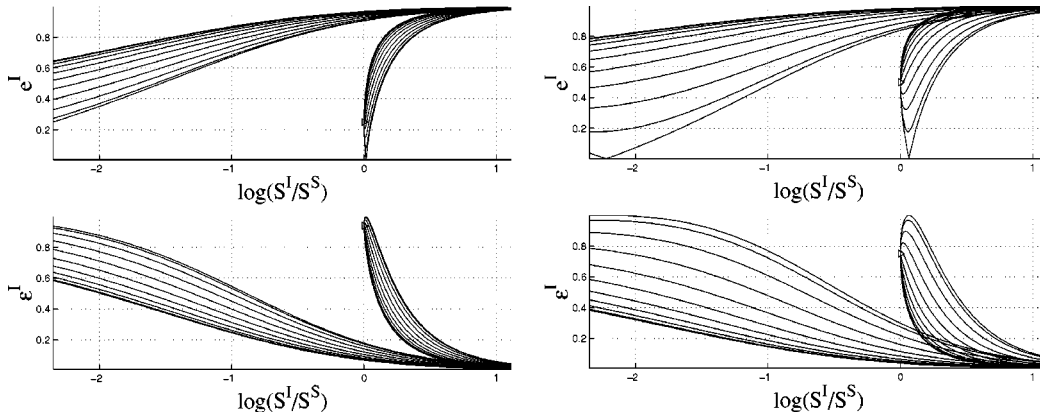


FIG. 7. Set of all morphologies ( $S^I, e^I$ ) of the image of a source of ellipticity  $e^S=0.25$  (left) and  $e^S=0.5$  (right). As explained in the text, we see (upper right plot) that there always exist two circular images, one for a subcritical transformation ( $\gamma = \gamma_- < 1$ ) and one for a critical transformation ( $\gamma = \gamma_+ > 1$ ) [see Eq. (117)]. The triangles represent the images by the transformation with  $\gamma=0$ .

Eq. (75) we only showed that  $\kappa$  vanishes in all directions such that the light ray arriving with this direction does not intersect the string world sheet. In this section, we are mainly interested in objects which do not overlap the string such that their deformation is the one with a  $\kappa=0$  field. Another restriction of this study is that we assume that the characteristic size of the object is smaller than the characteristic size of the variation of the shear  $\gamma$ ; thus we do not consider galaxies lying in the immediate neighborhood of the string (see Ref. [28] for an illustration). With these restrictions, we can consider that the deformation field has a zero convergence and the goal of this section is to study the main phenomenological properties of such a field. The two kinds of questions we would like to answer are as follows

(1) Given a source of surface  $S^S$  and ellipticity  $e^S$ , what can we say about the morphologies of all its possible images?

(2) Given two objects, how can we know that they are the images of the same source? This question reduces to studying the allowed morphologies of the sources that have the same images.

We start by setting the general framework and then study, respectively, questions (1) and (2). This study is a first step toward the discrimination between pairs of lensed sources by a cosmic string and fake lenses [26,27]. This study is made within the assumption that the shear variations over observed background images is small. It may actually be a severe limitation for such an approach if the string energy density is small.

### A. Describing the morphology of a cosmic object

To any object of elliptic shape such as a galaxy or a cluster, we can associate a positive definite symmetric matrix  $M_{ab}$  describing its shape as

$$X^T M X \leq 1, \quad (102)$$

where  $X^T = (x_1, x_2)$ . This matrix can be diagonalized as

$$M = P^T(\theta) \begin{pmatrix} \lambda_+ & 0 \\ 0 & \lambda_- \end{pmatrix} P(\theta), \quad (103)$$



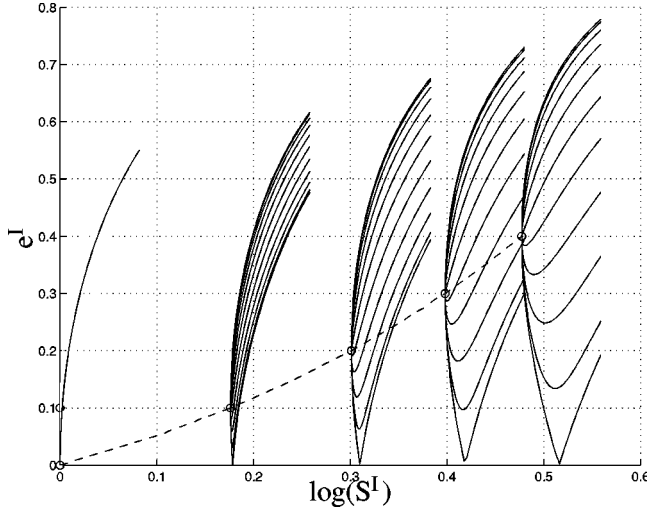


FIG. 8. The images of the different sources of respective shape  $(1,0)$ ,  $(1.5,0.1)$ ,  $(2,0.2)$ ,  $(2.5,0.3)$ ,  $(3,0.4)$  for a small deformation  $0 < \gamma < 0.3$ . The circles represent the image by the transformation  $\gamma = 0$ .

where  $P$  is a rotation matrix defined by

$$P(\theta) \equiv \begin{pmatrix} \cos \theta & \sin \theta \\ -\sin \theta & \cos \theta \end{pmatrix} \quad (104)$$

and a superscript  $t$  denotes the transposition.  $\lambda_- \leq \lambda_+$  are the two positive eigenvalues of  $M$  and  $\theta$  is an angle describing the orientation of its principal axis with respect to the basis  $n_a^\mu$ . Thus any object can be characterized by the set  $(\theta, \lambda_-, \lambda_+)$  from which we can define the surface  $S$  and ellipticity  $e$  of the object, respectively, as

$$S(M) \equiv \det(M) = \lambda_+ \lambda_-, \quad (105)$$

$$e(M) \equiv \frac{\lambda_+ - \lambda_-}{\lambda_+ + \lambda_-} = \sqrt{1 - 4 \frac{\det(M)}{[\text{tr}(M)]^2}} \quad (106)$$

and we also define  $\epsilon$  as

$$\epsilon \equiv 1 - e^2 = 4 \frac{\det(M)}{[\text{tr}(M)]^2}. \quad (107)$$

These definitions can indeed be inverted to get the two eigenvalues in terms of  $e$  and  $S$  as

$$\lambda_{\pm}^2 = S \left( \frac{1+e}{1-e} \right)^{\pm 1}. \quad (108)$$

Following Mellier [44], the ellipticity must be bounded by

$$\epsilon \gtrsim 0.5 \Leftrightarrow e \lesssim 0.71. \quad (109)$$

In the following, we will not be interested in the orientation of the object and we then define the *shape* as being the set  $(S, e)$ . The shape matrix  $M^I$  of any image can be related to the shape matrix  $M^S$  of its associated source as (see, e.g., Ref. [44])

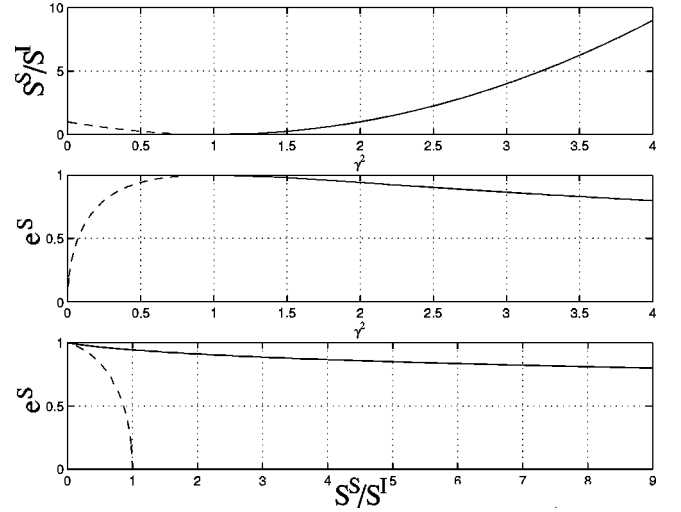


FIG. 9. Sources of a circular image. We show the variation of  $S^S/S^I$  (upper panel) and of  $e^S$  (middle panel) with respect to the strength of the deformation  $\gamma$ . The two branches correspond, respectively, to transformations such that  $\gamma < 1$  (dash line) and  $\gamma > 1$  (solid line).

$$M^I = \mathcal{A}^{-1} M^S \mathcal{A}^{-1} \quad (110)$$

(this is valid only if we consider that the characteristic size of the source is smaller than the characteristic size associated with the variation of the shear). Decomposing  $M^S$  as in Eq. (103) and introducing  $\tilde{M}^I \equiv P M^I P^t$  which represents the same shape as  $M^I$  after a rotation of  $-\theta$ , we obtain that

$$\tilde{M}^I = (P \mathcal{A}^{-1} P^t) \begin{pmatrix} \lambda_+ & 0 \\ 0 & \lambda_- \end{pmatrix} (P \mathcal{A}^{-1} P^t). \quad (111)$$

Thus,  $\tilde{M}^I$  is the image of the source  $\tilde{M}^S \equiv \begin{pmatrix} \lambda_+ & 0 \\ 0 & \lambda_- \end{pmatrix}$  by the transformation

$$\tilde{\mathcal{A}}^{-1} \equiv P \mathcal{A}^{-1} P^t = \frac{1}{1 - \tilde{\gamma}^2} \begin{pmatrix} 1 + \tilde{\gamma}_1 & -\tilde{\gamma}_2 \\ -\tilde{\gamma}_2 & 1 - \tilde{\gamma}_1 \end{pmatrix}$$

with

$$\tilde{\gamma} = P(-2\theta) \tilde{\gamma}. \quad (112)$$

As long as we are interested only on the shape (i.e., surface and ellipticity) of the sources and/or images, we always can choose one of them to be diagonal.

### B. Morphology of the images of a given source

From the previous analysis, we can conclude that, if we are not interested in the relative orientation of the source and of the image, we can just restrict the problem by considering the source and the transformation matrix to be given by

$$M^S = \begin{pmatrix} \lambda_+ & 0 \\ 0 & \lambda_- \end{pmatrix}, \quad \mathcal{A}^{-1} = \frac{1}{1 - \gamma^2} \begin{pmatrix} 1 + \gamma_1 & -\gamma_2 \\ -\gamma_2 & 1 - \gamma_1 \end{pmatrix}. \quad (113)$$

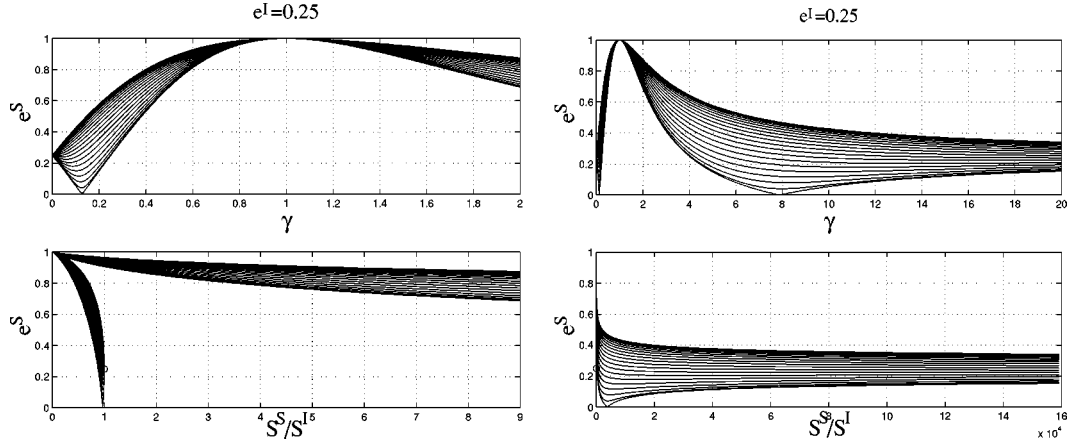


FIG. 10. Variation of the ellipticity of the source of an image of ellipticity  $e^I=0.25$ . The circles represent the deformation with  $\gamma=0$ .

Setting

$$\vec{\gamma} \equiv \gamma \begin{pmatrix} \cos \alpha \\ \sin \alpha \end{pmatrix} \quad \text{with } \gamma \geq 0 \text{ and } \alpha \in [0, 2\pi], \quad (114)$$

we can easily show that the shape  $(S^I, e^I)$  of the image is related to the one of the source  $(S^S, e^S)$  by

$$S^I = \frac{1}{(1 - \gamma^2)^2} S^S, \quad (115)$$

$$\epsilon^I = \frac{(1 - \gamma^2)^2}{(1 + \gamma^2 + 2\gamma e^S \cos \alpha)^2} \epsilon^S, \quad (116)$$

where  $\epsilon$  is defined in Eq. (107). In the case of a circular source ( $e^S=0$ ) we deduce that, since  $(S^I/S^S, e^I)$  depends only on  $\gamma$ , (i) two images of same surface have same ellipticity and that (ii) all the images lie on a curve in the plane  $(S^I/S^S, e^I)$ . In Fig. 6, we depict the variation of  $S^I$  and  $e^I$  in function of  $\gamma$  and the ensemble of the images of a circular source.

In the general case ( $e^S \neq 0$ ) we can determine all the morphologies of the images of a given source in the plane  $(S^I/S^S, e^I)$ . In Fig. 7, we depict these sets, respectively, for  $e^S=0.25$  and  $e^S=0.5$ . We note that all the curves have the same asymptote  $(S^I/S^S)=\infty, e^I=1$  which is reached when  $\gamma=1$ , i.e., on the critical line; on these points, the amplification  $\mu \equiv [\det(\mathcal{A})]^{-1}$  is infinite. Whatever  $e^S$ , there exist always two circular images (i.e., such that  $\epsilon^I=1$ ) obtained for

$$\gamma_{\pm} = \frac{e^S}{1 \pm \sqrt{\epsilon^S}}, \quad \alpha \equiv \pi[2\pi] \quad (117)$$

(the condition on  $\alpha$  is obtained from the requirement that  $\gamma > 0$ ; there are also two solutions for  $\alpha \equiv 0[2\pi]$  but they lead to negative values of  $\gamma$ ). Now, since from Eq. (115)  $S^I_+/S^I_- = (1 - \gamma_-^2)^2 / (1 - \gamma_+^2)^2$ , the measure of the area of two such circular images enables us (i) to determine the ellipticity  $e^S$  of their common source and (ii) the shears  $\gamma_{\pm}$  of

the two deformations. Indeed the bound on the ellipticity (109) has to be fulfilled by  $e^S$  and this can be a test to reject fake pairs of images.

In the more general case of a pair of non circular images, one cannot reconstruct the ellipticity of their source but we can still conclude from the ratio of their surfaces if they correspond to transformations  $\vec{\gamma}_1$  and  $\vec{\gamma}_2$  that are both subcritical ( $\gamma_1 < 1$  and  $\gamma_2 < 1$ ) or where one is critical and the other subcritical ( $\gamma_1 < 1$  and  $\gamma_2 > 1$ ).

For small deformations ( $\gamma \ll 1$ ), we have that

$$S^I/S^S \approx 1 + 2\gamma^2 + \mathcal{O}(\gamma^4), \quad (118)$$

$$\epsilon^I/\epsilon^S \approx 1 - 4e^S \cos \alpha \gamma + 4[3(e^S)^2 \cos^2 \alpha - 1]\gamma^2 + \mathcal{O}(\gamma^3) \quad (119)$$

so that the images almost lie on a parabola centered on  $(S^I, e^I) = (S^S, e^S)$  (see Fig. 8). In such a weak field, two images of the same object will have almost the same surface but can have very different ellipticities.

### C. Morphology of possible sources of a given image

We now ask the reverse question: given an image  $(S^I, e^I)$ , from which set of sources can it be the image? Following the description and notations of the two previous sections, we now set

$$M^I = \begin{pmatrix} \lambda_+ & 0 \\ 0 & \lambda_- \end{pmatrix}, \quad \mathcal{A} = \begin{pmatrix} 1 - \gamma_1 & \gamma_2 \\ \gamma_2 & 1 + \gamma_1 \end{pmatrix} \quad (120)$$

from which we deduce that, since  $M^S = \mathcal{A} M^I \mathcal{A}$ , the shape of the source is related to the one of its images by

$$S^S = (1 - \gamma^2)^2 S^I, \quad (121)$$

$$\epsilon^S = \frac{(1 - \gamma^2)^2}{(1 + \gamma^2 - 2\gamma e^I \cos \alpha)^2} \epsilon^I. \quad (122)$$

As a first exercise, we depict on Fig. 9 the sources  $(S^S, e^S)$  of a circular image ( $e^I=0$ ). The ellipticity of the sources (109)

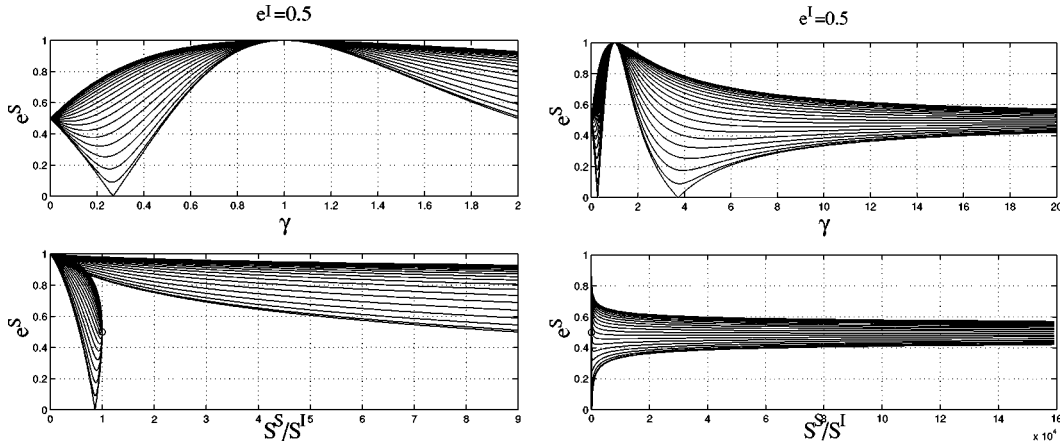


FIG. 11. Variation of the ellipticity of the source of an image of ellipticity  $e^I=0.25$ . The circles represent the deformation with  $\gamma=0$ .

and on the strength of the deformation  $\gamma$  may enable us to extract from such a plot informations about the source of a circular image.

In the general case where  $e^I \neq 0$ , we can reconstruct all the morphologies of the source that can lead to the observed image. As an example we depict such sets in the two cases where  $e^I=0.5$  and  $e^I=0.25$ , respectively, on Figs. 10 and 11. We note that all the curves pass through the point  $(S^S, e^S) = (0, 1)$  which is reached when  $\gamma=1$ , i.e., on the critical line. Again, one can sort out that any object can be the image of two circular sources obtained by the two transformations

$$\gamma_{\pm} = \frac{e^I}{1 \mp \sqrt{e^I}} \quad \alpha \equiv 0[2\pi] \quad (123)$$

and the measure of  $(S^I, e^I)$  enables us to determine  $\gamma_{\pm}$  and the two surfaces  $S^S_{\pm}$ .

If one measures the shape of two images  $(S^I_1, e^I_1)$  and  $(S^I_2, e^I_2)$  one can reconstruct, as in Figs. 10 and 11, the set of morphologies of their possible sources. Given bounds on  $e^S$ , as in Eq. (109), and on  $\gamma$  one can figure out graphically if these two observations are likely to be images of the same object. Indeed for very weak deformations ( $\gamma \ll 1$ ) one gets that two images of the same object must have almost the same surface but can have very different ellipticity (see Fig. 12 where we have plotted the source shapes of objects of different shape for small deformation).

## VI. CONCLUSION

We have considered the general lensing properties of objects such as cosmic strings where relativistic motions and nontrivial equation of state induce metric perturbations of all sorts. We demonstrated that the deformation field of a string system on the image plane is the same as the one of a static linear distribution of matter projected on the photon trajectory. A consequence of this result is that the deformation field has a vanishing convergence ( $\kappa=0$ ) everywhere but on the projection of the intersection of the observer past light cone and the string world sheet. We explicitly illustrate this result with the case of a circular cosmic string loop in a plane

perpendicular to the line-of-sight for which we generalize the results found in Ref. [24] to string with any equation of state. We also showed that (i) the fact that the deformation field outside the loop is equivalent to the one obtained by a massive point and (ii) that a light ray passing inside the loop is not deflected are due to the energy conservation of the string.

We also paid attention to the validity of thin lens approximation for this unusual lens system. This approximation is discussed in detail through the case of a static tilted straight cosmic string. It lead us to point out that for string with a general equation of state, the deflection may be more important than for a Goto-Nambu string, this being understood by the fact that the stress-energy tensor of a general cosmic string can always be decomposed as the superposition of a Goto-Nambu string and a lineic distribution of nonrelativistic matter. The deflection is then due to the combined effect of the deficit angle of the Goto-Nambu string and of the curvature induced by the lineic distribution of matter.

We also studied general phenomenological consequences of deformation fields with zero convergence on multiple im-

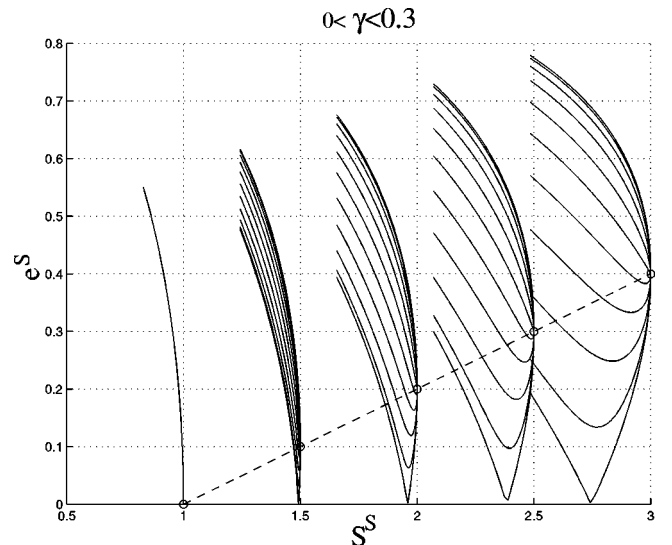


FIG. 12. The source shapes of different images of respective shape  $(1,0)$ ,  $(1.5,0.1)$ ,  $(2,0.2)$ ,  $(2.5,0.3)$ ,  $(3,0.4)$  for a small deformation  $0 < \gamma < 0.3$ . The circles represent the deformation  $\gamma=0$ .

age systems, the main goal being to be able to assess if two images are likely to form an image pair of the same source. For that purpose, we derived all the image shapes of a given source as well as all the source shapes of a given image. These results may serve as a groundwork for the elaboration of string detection strategies.

We are aware that this latter part is limited by the fact that we only took advantage of the zero-convergence property. In practice more intricate distortion properties of the images are likely to be useful. This is one of the aims of the companion

paper [28] where more quantitative phenomenological properties are presented that take into account local string energy fluctuations.

### ACKNOWLEDGMENTS

We would like to thank Ruth Durrer, Yannick Mellier, Patrick Peter, and Albert Stebbins for discussions on the subject.

- 
- [1] T. W. B. Kibble, *J. Math. Phys. A* **9**, 1387 (1976).
  - [2] N. D. Mermin, *Rev. Mod. Phys.* **51**, 591 (1979).
  - [3] P. Peter, *Phys. Rev. D* **46**, 3322 (1992).
  - [4] A. Vilenkin and P. Shellard, *Cosmic Strings and Other Topological Defects* (Cambridge University Press, Cambridge, England, 1994).
  - [5] M. Hindmarsh and T. W. B. Kibble, *Rep. Prog. Phys.* **48**, 477 (1995).
  - [6] R. Durrer, *New Astron. Rev.* **43**, 111 (1999).
  - [7] N. Turok, U.-L. Pen, and U. Seljak, *Phys. Rev. D* **58**, 023506 (1998).
  - [8] A. Albrecht, R. A. Battye, and J. Robinson, *Phys. Rev. D* **59**, 023508 (1999).
  - [9] R. Durrer, M. Kunz, and A. Melchiorri, *Phys. Rev. D* **59**, 123005 (1999).
  - [10] J.-P. Uzan, N. Deruelle, and A. Riazuelo, in *Texas Symposium on Relativistic Astrophysics and Cosmology*, Proceedings of the 19th Symposium, Paris, France, 1998, edited by E. Aubourg *et al.* [*Nucl. Phys. B (Proc. Suppl.)* **80** (2000)].
  - [11] N. Kaiser and A. Stebbins, *Nature (London)* **276**, 391 (1984).
  - [12] K. Benabed and F. Bernardeau, astro-ph/9906161.
  - [13] J.-P. Uzan and P. Peter, *Phys. Lett. B* **406**, 20 (1997).
  - [14] A. Vilenkin, *Phys. Rev. D* **23**, 852 (1981).
  - [15] A. Vilenkin, *Astrophys. J., Lett. Ed.* **282**, L51 (1984).
  - [16] A. Vilenkin, *Nature (London)* **322**, 613 (1986).
  - [17] J. R. Gott III, *Astrophys. J.* **288**, 422 (1985).
  - [18] C. Hogan and R. Narayan, *Mon. Not. R. Astron. Soc.* **211**, 575 (1984).
  - [19] M. Hindmarsh, in *The Formation and Evolution of Cosmic Strings*, edited by G. W. Gibbons, S. W. Hawking, and T. Vachaspati (Cambridge University Press, Cambridge, England, 1990), p. 527.
  - [20] M. Hindmarsh and A. Wray, *Phys. Lett. B* **251**, 498 (1990).
  - [21] P. Peter, *Class. Quantum Grav.* **11**, 131 (1994).
  - [22] J. Garriga and P. Peter, *Class. Quantum Grav.* **11**, 1743 (1994).
  - [23] A. A. de Laix, *Phys. Rev. D* **56**, 6193 (1997).
  - [24] A. A. de Laix and T. Vachaspati, *Phys. Rev. D* **54**, 4780 (1996).
  - [25] A. A. de Laix, L. M. Krauss, and T. Vachaspati, *Phys. Rev. Lett.* **79**, 1968 (1997).
  - [26] L. L. Cowie and E. M. Hu, *Astrophys. J., Lett. Ed.* **318**, L33 (1987).
  - [27] E. M. Hu, *Astrophys. J. Lett.* **360**, L7 (1990).
  - [28] F. Bernardeau and J.-P. Uzan, following paper, *Phys. Rev. D* **63**, 023005 (2001).
  - [29] C. W. Misner, K. S. Thorne, and J. A. Wheeler, *Gravitation* (Freeman, San Francisco, 1973).
  - [30] R. K. Sachs, *Proc. R. Soc. London A* **264**, 309 (1961).
  - [31] P. J. E. Peebles, *Principles of Physical Cosmology* (Princeton University Press, Princeton, 1993).
  - [32] P. Schneider, J. Ehlers, and E. E. Falco, *Gravitational Lenses* (Springer-Verlag, Berlin, 1992).
  - [33] S. Seitz, P. Schneider, and J. Ehlers, *Class. Quantum Grav.* **11**, 2345 (1994).
  - [34] L. Schwartz, *Théorie des Distributions* (Hermann, Paris, 1968).
  - [35] R. Durrer, *Phys. Rev. Lett.* **72**, 3301 (1994).
  - [36] T. Futamase and M. Sasaki, *Phys. Rev. D* **40**, 2502 (1989).
  - [37] R. K. Sachs and A. M. Wolfe, *Astrophys. J.* **147**, 73 (1967).
  - [38] B. Carter, M. Sakellariadou, and X. Martin, *Phys. Rev. D* **50**, 682 (1994).
  - [39] B. Carter, in *Formation and Interactions of Topological Defects*, edited by A.-C. Davis and R. Brandenberger (Plenum Press, New York, 1995).
  - [40] T. Goto, *Prog. Theor. Phys.* **46**, 1560 (1971); Y. Nambu, in *Symmetries and Quark Model*, edited by R. Chand (Gordon and Breach, New York, 1970), p. 269.
  - [41] N. K. Nielsen, *Nucl. Phys.* **B167**, 249 (1980); N. K. Nielsen and P. Olesen, *ibid.* **B261**, 829 (1987).
  - [42] E. Witten, *Nucl. Phys.* **B249**, 557 (1985).
  - [43] A. Stebbins, *Astrophys. J.* **327**, 584 (1988).
  - [44] Y. Mellier, *Annu. Rev. Astron. Astrophys.* **37**, 127 (1999).